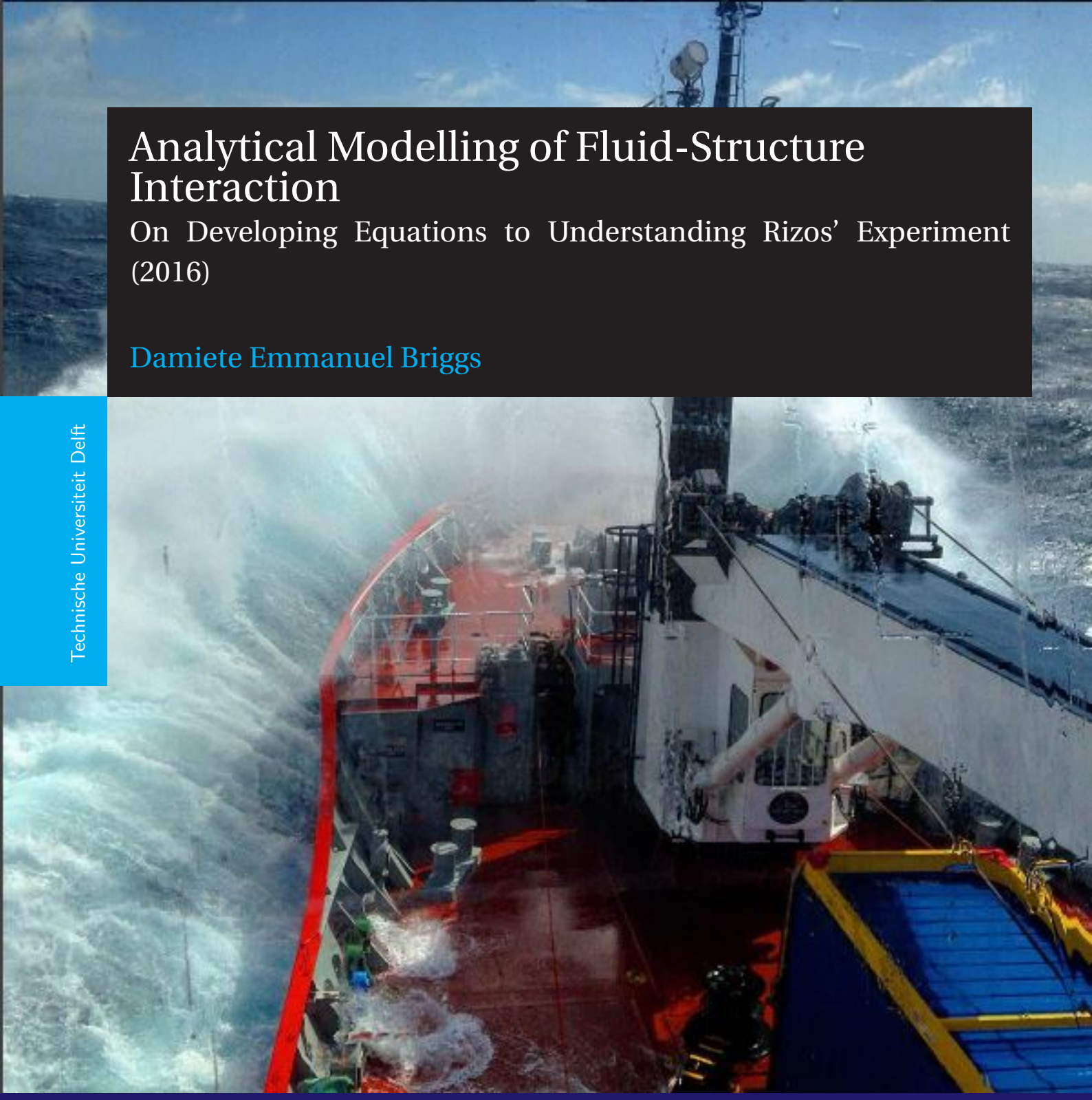

# Analytical Modelling of Fluid-Structure Interaction

## On Developing Equations to Understanding Rizos' Experiment (2016)

Damiete Emmanuel Briggs

Technische Universiteit Delft

TU Delft Delft University of Technology

Challenge the future

# Analytical Modelling of Fluid-Structure Interaction

## On Developing Equations to Understanding Rizos' Experiment (2016)

by

**Damiete Emmanuel Briggs**

in partial fulfillment of the requirements for the degree of

**Master of Science**
in Offshore and Dredging Engineering

at the Delft University of Technology,
to be defended publicly on Wednesday August 30, 2017 at 10:00 AM.

| | | |
|---|---|---|
| Supervisor: | Dr. ir. P. R. Wellens | |
| Thesis committee: | Prof. dr. ir. A. P. van 't Veer, | TU Delft |
| | Dr. ir. P. R. Wellens, | TU Delft |
| | Ir. k. Visser Rear-Admiral(ME)ret, | TU Delft |

An electronic version of this thesis is available at http://repository.tudelft.nl/.

TU Delft Delft University of Technology

# *Acknowledgements*

I will have to say that I am simply a make-up of the giants on whose shoulders I have stood on to help me go further in life. First of all, I would like to thank the Almighty GOD, my creator who daily helps me and blesses my mind with inspiration. I would also like to express my sincere gratitude to my supervisor Dr.ir. Peter Wellens, for his guidance, insightful comments and continuous support offered during my M.Sc thesis.

Besides my supervisor, I would love to thank my colleauges: especially Femiwa Olajide, Joost van den Bosch who were always ready to listen to me and brainstorm with me in my hiccups days, to Ratnakar Gadi who took special interest in me and my thesis always providing solicited and unsolicited help during my M.Sc thesis. To Emeric Descourtieux who always asked critical questions and helped me to put finishing touches to setting-up my MAPLE model, to my favourite *Nederlander*, Fabian J. Koppes who created the time to vet my MATLAB program and give insightful methods to help. To Dan Shekwomwaza (Chief Dan) for his selfless support and critical attitude towards proof-reading my thesis report and gave helpful feedbacks.

I want to specially thank my unsung heroes: Sahil Sharma, Alden Antony Louis(King Louis), Semipe Oyedokun, Marcel Mbene, Dimitris Ntrou, Kostas Kiskiras, Seun Balogun and my American Cody Owen. To my 'sheroes': Lena Bakaloni, Charlotte Schiottz Hassings, Victoria Obayemi and Stephanie Apochi. They were all helpful in spreading their best wishes and goodwill towards me.

Finally to my family, my aunt Soibifaa Briggs, who convinced me to come study in The Netherlands, My Dad, Priye Briggs (M.D) my number one fan, personal doctor turned construction engineer who was always ready to listen to my victories and failures during my post-graduate studies and always on stand-by to share life lessons with me (informal training), to my mum, Ngoba Briggs and granny, RoseMary Briggs, for their immense support and prayers.

*Damiete Emmanuel Briggs*

*Delft, August 2017*

# *Abstract*

The activities of humans in the marine environment are on a steady rise; this trend follows the exposure of offshore structures and vessels to harsh environmental conditions. On the other hand, there is continuous demand for lighter, faster and more efficient vessels. Technological advancement in composite materials and better design methods invariably leads to more sophisticated computational tools. In these tools, the inherent flexibility of the structure is involved in the calculation of its loading and response – introducing the aspect of fluid-structure interaction. However, more than fluid-structure interaction, hydroelasticity which is a subset of fluid-structure interaction allows for deformation of the structures due to fluid. Current industry practice neglects these deformations and all structures are designed as rigid bodies. These practices lead to overestimation of the frequency – which translates to the mass and how stiff the structure is. Design based on hydroelasticity allows for knowing the true behaviour of the structure; thus, a coupling of fluid and structure yields a true appreciation of these designs. The objective of this study is to formulate and solve analytically the coupling phenomenon behind fluid-structure interaction.

An experiment designed by Lampros Rizos in 2016 which modelled fluid-structure interaction consisted of a set-up with a cylinder immersed in a larger cylindrical tank. The immersed cylinder having a flexible circular membrane (structure) located at its bottom. The cylinders were filled with non-viscous liquid and exhibited free surface.

The designed experiment was decoupled and a systematic build up in understanding the dynamics of all components – structure and fluid were solved. Firstly, the dynamics of the structure when dry (In vacuo) was idealized in 2-D and 3-D. Secondly, the system was coupled and solved in 2-D and 3-D when structure is located at the top and bottom of a single cylinder individually. The use of a series solution: Fourier-Cosine and Fourier-Bessel series solutions were used for 2-D and 3-D cases respectively. Along with these series solutions, the fluid governing equations were employed to solve for the coupled frequencies. Lastly, the entire submerged structure was analysed and solved.

The hydroelastic or coupled frequencies and vibration patterns are determined for lower angular and radial modes for which the influences of various parameters are investigated. A trend was observed – that for lower modes, the hydroelastic frequencies are lower than individual membrane natural frequencies at low frequencies. At higher frequencies, the coupling effects are larger making the coupled frequency higher than uncoupled frequencies. There is a strong relationship between the tension of the membrane and the hydroelastic frequencies. An increase in the tension causes an increase in the hydroelastic frequencies. Also, the hydroelastic frequencies increase as the fluid depth increases. More so, the increase in fluid depth tends to converge towards the uncoupled fluid free-surface frequency. The comparison of the analytical solution with experimental and numerical solutions does not match perfectly and thus, further works to improve this study are recommended

# CONTENTS

# LIST OF FIGURES

# LIST OF TABLES

# LIST OF NOMENCLATURE

| | |
|---|---|
| a | radius of membrane |
| $\alpha$ | coefficient of amplitude membrane when located at the bottom |
| b | length of rectangular container |
| $c$ | speed of wave |
| A,B,C,D | abitrary constants representing amplitude of the string *In Vacuo* |
| $A_0$,$A_n$,$B_0$,$B_n$ | abitrary constants representing amplitude of the fluid velocity potential in 3-D case |
| $A_d$ | abitrary constants representing amplitude of fluid velocity potential in 2-D case |
| $A_f$,$B_f$,$D_f$ | abitrary constants representing amplitude of string displacement in general solution |
| $\epsilon$ | variable for space in string |
| $\psi$ | coefficient of amplitude membrane located at the top |
| $\xi$ | coefficient of amplitude when is submerged |
| $k_n$, k | wave number of velocity potential of 3-D and 2-D respectively |
| $\kappa$ | variable of time |
| $l$ | length of string |
| $\lambda$ | non-dimensional frequency parameter of membrane in *In Vacuo* |
| m | nodal circle |
| $m_m$, $m_s$ | mass of membrane and string respectively |
| $\mu$ | non-dimensional coupled frequency parameter of membrane |
| n | nodal diameters and order of Bessel function |
| E,F,G,$H_{m_m}$, I, $L_n$,M,N | abitrarty constants representing amplitudes of membrane dynamics |
| $J_n$ | Bessel function of $n_{th}$ order |
| p | abitrary constant representing a periodic frequency |
| P | dynamic pressure of the fluid |
| $T_o$, T | tension of membrane and string respectively |
| r, $\theta$, z | coordinate axis of membrane |
| $w$ | displacement of the membrane |
| x,z | coordinate axis of 2-D case |
| $\rho$, $\rho_s$ | density of fluid and string respectively |
| $\phi$ | velocity potential of fluid |
| $\upsilon$ | mass parameter for 2-D case |
| X,Y | kinectic and potential energy respectively |
| $\omega$ | natural frequency of string |
| $\omega_s$ | fluid free surface frequency |
| $\omega_c$ | coupled frequency of fluid and structure |

# 1

# INTRODUCTION

## 1.1. BACKGROUND INFORMATION

Issues regarding vibration cuts across many multidisciplinary engineering fields such as civil, marine, mechanical, acoustics and aerospace. Examples of vibration problems in these fields are: wind loads on the cables of a suspension bridge and earthquakes, wave loading in offshore platforms and marine vehicles, pressure waves in flexible tubes, dynamics of percussion instruments, aero-elastic modelling of aircraft wings and wind turbine blades, to mention but a few. Human beings regard these vibrations as uncomfortable and thus over the years, engineers have come up with solutions to reduce these vibrations. In modern engineering, there is a growing trend towards thinner and lighter structures, this is due to a combination of modern design methods and developments of composite materials. This trend will invariably lead to flexible structures. As regarding the marine environment, flexibility of the structure yields to a structure-liquid interaction of an elastic nature. No matter the size of a structure ranging from large-capacity containers for liquid storage to medium and small sized propellant containers for missiles, space vehicles or satellite, the knowledge of the natural frequencies of the elastic structure and the fluid considered individually is not enough for proper design of the overall system. Thus, understanding the overall behaviour of the system is needed. Fluid-Structure Interaction (FSI) is simply the coupling of solids and fluids that share a common interface. However, hydro-elasticity is a branch of FSI concerned with the motions of deformable bodies through liquids usually an elastic solid structure.

In current practice, in order to predict the effect of wave loads on marine structures, interaction between structural vibrations and hydrodynamic forces are neglected. Additionally, the dynamic properties of marine structures in coupling between motions of structure and hydrodynamic forces are neglected. This has led to many conservative designs in the industry based on the assumptions of rigid body motions. Hydro-elastic based design desires to incorporate this cause and effect phenomenon between hydrodynamic forces on the motion and dynamics properties of marine structure in predictive response. Also, there is a growing demand for larger structures capable of carrying more loads at a higher speed with minimum vibration level as safety, workability and environmental criteria become stringent. In order to be able to represent these large structures as well as capture the coupling phenomenon, Adhikari[5] suggests the use of mathematical models. However, this interaction is difficult to capture as the mathematical theory of hydro-elasticity and the mathematical methods for solving such complex theory is not easily represented. This is due to the complexity of dynamic and kinematic properties of both domain, largely because fluid and elastic nature of structural deformations are dependent on hydrodynamic forces and vice-versa. An example of the push towards modern trends is the increase in dimensions of structural bodies such as floating vessels, oil containers and cargo ships, which results to a decrease in overall stiffness leading to natural

frequencies so low, that the vessels are near exciting frequencies of environmental forces which can cause excessive vibrations to the vessel. More so, the approach of rigid body modelling leads to more severe structural response due to overestimation of the water pressure Helder and Bunnik [6].

Modern problems in FSI includes:

- Slamming problems: The design of marine structures such as ships and other floating structures, its environmental loads are traditionally considered as rigid bodies. This is considerable to a certain motion response level. Beyond this level, the response of such structure must account for its flexibility. Motion responses such as global springing, whipping vibratory response of ship and local hydro-elastic effects relating to sloshing of Liquefied Natural Gas (LNG) tanks are examples of FSI problems. Additionally, water entry problems on the bow of the ship behaves like a wave impact onto a flexible wall [7].

- Hydro-elastic waves: Hydro-elastic waves generated by moving ice, ocean waves and sea-ice interaction are problems arising from non-linearities which further research is done upon. The scattering of waves by cylinders, vertical and floating elastic plates are a growing concern [5].

- FSI: In other fields such as biomedical engineering, examples regarding the elastic capsules in channel and swimming mechanics in the body. Also, the storage of $CO_2$ at the bottom of the ocean, negative damping in ice engineering are considerable growing concerns in FSI [7].

- FSI: In the energy industry, the use of structures such as flexible risers, marine pipelines and electric cables in offshore wind exhibits FSI problems which on-going research is done upon [7].

Attention is needed in this rapidly growing field of study, owing to the expansion of human activities in the marine environment. The need for less expensive vessel design and in-depth knowledge to capture this phenomenon is important. Hence, there is a need for collaborative effort from research and industry partnership.

FSI problems in the field of acoustics have been investigated extensively. For example, analytical models of dynamics of percussion instruments such as the drum head. Flexible membrane and plates are also commonly used in mathematical models of structures when conducting research in FSI. Also, air and water are commonly used fluid in FSI is study.

## 1.2. ANALYTICAL AND NUMERICAL METHODS OF SOLVING FSI PROBLEMS

The FSI phenomenon is characterised by its complexity and multidisciplinary nature in scientific and engineering domains. Hence, there is much need for wide development in this area. A great deal of knowledge has been understood about the individual characteristics of this phenomenon but not the coupling effect. The shared boundaries of the structure and fluid say a lot about how to go about the design of these coupling effect. Considering only structure, the boundary conditions commonly used for the flexible structure are: clamped, simply supported edges and free edges. The boundary conditions used for fluid are known as the governing equations, consisting of Laplace equation, free surface conditions and seabed condition. A major step in understanding these coupling phenomenon is in the critical study of the fluid-structure shared boundaries. The interface where the structure and fluid must be incorporated into the holistic design.

In other to reduce the complexity of the problem, it is often easier to capture the effects of clamped edges. According to Leissa[8], a clamped boundary condition has its frequencies independent of the Poisson ratio, which is not the case for other boundary conditions such as free edges and simply supported edges. The Poisson ratio is a property of the material and as displacement occurs, the frequency changes accordingly but for a clamped boundary condition, the displacements are assumed to be small. In the field of acoustics Leniowski[9] analysed the control of active vibration of circular fluid-loaded plate. Using the acoustic wave equation of Helmholtz, it was concluded that lengths of emitted waves are comparable with geometric size of the external source and finite baffle. In this study, the use of the Helmholtz equation is not applicable because the fluid being considered are incompressible, unlike in acoustics. However, the size of the structure affects the behaviour of the waves, which is expected.

When air and structure are involved Moosrainer and Fleischer[10] suggested that Boundary Element Method (BEM) be used to solve acoustic problems. Finite Element Method (FEM) is used to measure the structural coupling matrix due to the pressure loading of the fluid. The BEM comes to play because of the non-linear frequency dependence of the fluid matrix and it creates the so-called added mass to the coupled system. The natural frequencies and modal damping were obtained from the abscissas imaginary axis and real part respectively. No structural damping was considered and it was concluded that the first mode is dominant and eigen frequencies are only dependent on the volume of the kettle drum and not the shape. Which is strongly influenced by air loading. The air loading will affect the natural frequency of the system as the shape of the kettle drum due to the boundary conditions dictates how air velocity travels around the volume of the surface, the membrane(drum head) is not significant in this process. This method still suggests isolated methods in coupling the FSI.

Amabili[11] used the Rayleigh-Ritz methods that invokes kinetic and potential energy and in a rather interesting relationship with natural frequency. This leads to an eigen-value problem as the method suggests that coupled frequency of fluid and structure is a ratio of potential energy of plate to sum of kinetic energy of plate and fluid considering the plate is resting on the fluid. This is logical in the perspective that loading of pressure from the fluid can be defined by energy methods and following conservation of energy, these energy (kinectic and potential) are frequency dependent. Bhuta and Koval[12] worked on oscillations of a flexible plate and elastic membrane as the bottom of a rigid cylinder with rigid walls interacting with free liquid surface and concludes that the effect of the membrane on axisymmetric sloshing which is of interest to engineering application is particularly small and coupled frequencies were slightly smaller than that of a completely rigid cylinder.. The coupled natural frequency due to the flexible bottom is lower, however, an increase in tension of the membrane makes the frequency behave like a rigid structure. This is a logical conclusion, however, the mode shapes behaviour was difficult to comprehend.

Bauer and Chiba[13] and Bhuta and Koval[12] concluded that the effect of the coupling relies on the ratio of the height of the cylinder and the radius of the membrane, thus when this ratio is less than unity, the coupling effect is considerable, otherwise, the coupling is negligible. This is simply because the diameter of the cylinder is a representative of the wavelength ensued by the fluid where the height of the fluid column is a representative of the fluid depth. This ratio is the so called dispersion-relationship that determines how wave particles behave with respect to fluid depth and frequency.

In the last decade, computational tools to solving problems regarding FSI has attracted a lot of attention from different fields such as acoustic, aerospace, civil, mechanical and offshore engineering. In offshore engineering, the effects of free surface are most important and thus the physics that occurs must be captured in this computations. Moreover, the coupling motion and coupled responses of both domain(fluid flow and structure) needs to be well understood. Physical experiments are a means to validate the investigated processes. Generally, in FSI, three fluids used to de-

scribe the fluid domain are acoustic fluids, incompressible Navier-Stokes and compressible Navier-Stokes fluid Leniowska[9]. The easiest to model is the acoustic fluid since it is assumed that it is inviscid and can only transmits pressure waves. This is mainly because the radiation field generated by structure has negligible response on the surface velocity, but not the case for denser fluids like water. The other two types of fluids are modelled analytically with many assumptions which makes it complex, however modern numerical computational tools such as ComMotion[6] are being developed to solve this problem.

## 1.3. PROBLEM STATEMENT

### 1.3.1. JUSTIFICATION OF THE STUDY

An experimental set-up designed to capture this FSI problem using a thin circular membrane (similar) to a drum head[14]. The experiment is set up as: a membrane is submerged in between two cylinders of different dimensions, the first cylinder, smaller in dimensions (height and radius) have its bottom consisting of the clamped circular elastic membrane, with rigid side walls. The second cylinder is larger in dimensions (height and radius) have a rigid bottom and side walls. The two cylinders are exposed to free surface conditions. The level of the fluid is the same in both cylinders to cancel out hydrostatic effects Rizos [1]. This is shown in figure 1.1 below. The experiment was conducted without prior knowledge to understanding the theoretical representation of FSI. This thesis seeks to address this problem.

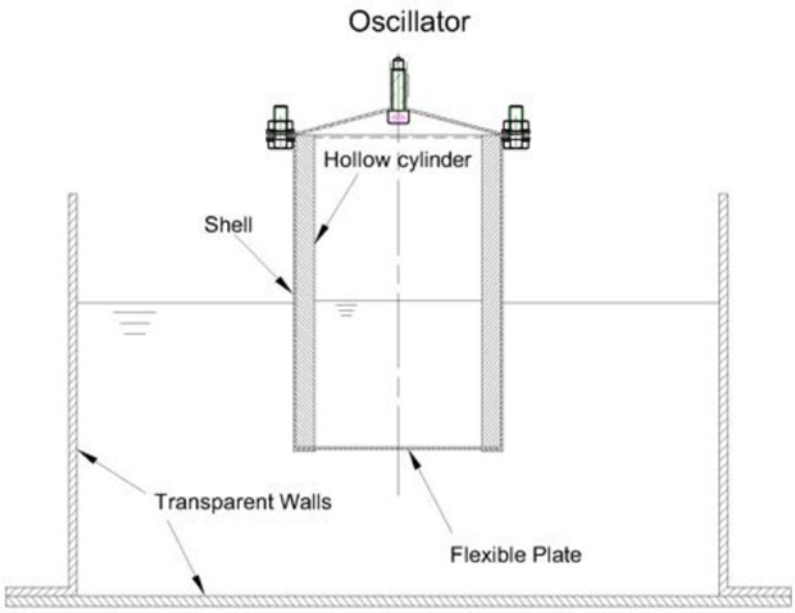


Figure 1.1: Experimental setup by Rizos [1]

A membrane is chosen instead of a plate to reduce the complexities in the analytical solution. The rationale is to reduce order of the mathematical differential equation. The non-linear characteristics of FSI problems and its wide range of application in the offshore engineering field needs further understanding for the appreciation of better designs of vessels and marine structures, also in prediction of motion and vessel response in operational campaigns.

### 1.3.2. RESEARCH OBJECTIVE

The required goal is to formulate and solve analytically the dynamics of a submerged membrane and fluid free surface FSI coupling phenomenon of the Rizos' experiment. To know the effects of the frequencies on the structure due to its coupling with the fluid and *vice-versa*, and to understand effect the vibration mode behaviour of the coupling frequency with respect to its properties of the membrane such as tension and height of the fluid column exposed to free surface condition.

# 2

# METHODOLOGY

## 2.1. INTRODUCTION

After several approaches reviewed for the investigation of FSI, the analytical solution to Rizos' experiment needs to be modelled. The technique was modelled in three parts, firstly, to understand the dynamics of the natural frequencies and vibration modes of the structure (string and circular membrane)without external excitation *In vacuo* (dry case). Secondly, to understand the dynamics of the coupled (fluid-structure interaction) system with captured free surface effects in 2-D using an elastic string as the structure and in 3-D using an elastic circular membrane. Finally, solving the entire problem captured by Rizos' experiment.

## 2.2. DYNAMICS OF A FREELY VIBRATING STRING *In Vacuo*

To understand the problem at hand, solving the problem is easier when broken down into bits, thus idealising the problem into a simple 2-D case is the way forward. The structure considered is a string.

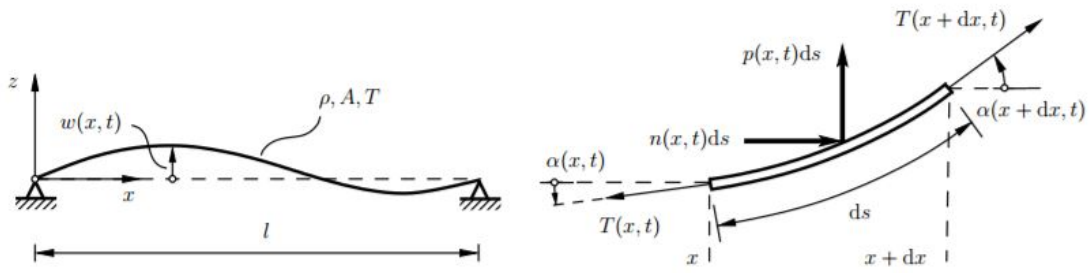


Figure 2.1: A taut string and infinitesimal string element [2]

where $\rho_s$ is the density of the string, $A_s(x)$ is the cross sectional area, $l$ is the length of the string, $T(x,t)$ is tension of the string, subject to distributed forces (N/m) and $w(x,t)$ is the transverse displacement of the string.

The equation of motion of a taut string follows the wave equation in 1-D since the dimension of the length of the string is greater than the other dimensions.

$$T\frac{\partial^2 w}{\partial^2 x} = \rho_s A_s \frac{\partial^2 w}{\partial^2 t} \tag{2.1}$$

With the boundary and initial conditions of the string given as

$$w(t) = 0 \quad |_{x=0\leq x\leq l}, \tag{2.2}$$

$$w(x) = 0, \quad \frac{\partial w}{\partial t} = 0 \quad \Big|_{t=0\leq x\leq l} \tag{2.3}$$

For a uniform string, $A_s(x) = A_s$ and thus, the equation (2.4)

$$\frac{\partial^2 w}{\partial^2 t} - c^2 \frac{\partial^2 w}{\partial^2 x} = 0 \tag{2.4}$$

where $c = \sqrt{\frac{T}{\rho_s A_s}}$ takes the dimension of the speed of the wave in (m/s) with boundary condition given as $w(0,t) = 0$ and $w(l,t) = 0$ .

In solving equation (2.4) above, the use of variable separable terms are used thus,

$$w(x,t) = \epsilon(x)\kappa(t) \tag{2.5}$$

this yields to equation (2.6)

$$c^2 \frac{\frac{d^2\epsilon}{dx^2}}{\epsilon} = \frac{\frac{d^2\kappa}{dt^2}}{\kappa} = \omega^2 \tag{2.6}$$

solving equation (2.6) yields

$$Time: \kappa(t) = A\cos(\omega t) + B\sin(\omega t) \tag{2.7}$$

$$Space: \epsilon(x) = C\cos(\iota x) + D\sin(\iota x) \tag{2.8}$$

$$\iota = \frac{\omega}{c} \tag{2.9}$$

A, B, C, D represents the amplitudes of the waves and it depends on the initial and boundary conditions.

The separation constant $\omega^2$ must be real to ensure the possibility of harmonic vibration, and it has a physical meaning of natural frequency of the string. In solving the space related part, the separation constant and the normal vibration modes are found.

From the space related solution, by substituting the boundary conditions shown in equation (2.3)

$$\epsilon(0) = 0, \quad C = 0 \tag{2.10}$$

$$\epsilon(l) = 0, \quad \sin(\iota l) = 0 \tag{2.11}$$

Thus, the natural frequency and vibration modes are given as

$$\iota_f l = f\pi, \quad \omega = c\iota_f = \frac{f\pi c}{l}, \quad f = 1,2,3,... \tag{2.12}$$

$$\epsilon_f(x) = D_f \sin(\iota_f x) = D_f \sin\left(f\frac{\pi x}{L}\right) \tag{2.13}$$

By substituting the boundary conditions given in equations (2.10) and (2.11), natural frequency and vibration modes given in equation (2.12) and (2.13), the general solution is obtained in equation (2.14)

$$w(x,t) = \sum_{f=1}^{\infty} (A_f \sin(\omega_f t) + B_f \cos(\omega_f t)) sin(\iota_f x) \tag{2.14}$$

## 2.3. DYNAMICS OF FREELY VIBRATING CIRCULAR MEMBRANE *In Vacuo*

The dynamics of a circular membrane such as a drum head or thin elastic sheet is particularly unique due to its geometry and boundary conditions [15]. Let the fixed coordinate axes $(r, \theta, z)$ be attached to the membrane as shown in figure 2.2. The assumption of this membrane are such that it has:

1. It is homogeneous which means density is constant.
2. It is subject to uniform in-plane tension force along its boundary condition.
3. It experiences small displacement in the vertical and transverse direction.
4. It is thin and flat.[1]

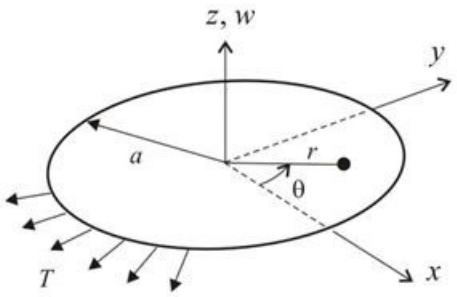


Figure 2.2: Analytical description of circular membrane [3]

It follows the wave equation as in 2-D in polar coordinates

$$T_o \nabla^2 w = m_m \frac{\partial^2 w}{\partial^2 t} \tag{2.15}$$

where

$$\nabla^2 = \frac{\partial^2}{\partial r^2} + \frac{1}{r}\frac{\partial}{\partial r} + \frac{1}{r^2}\frac{\partial^2}{\partial \theta^2} \tag{2.16}$$

$m_m$ is mass of membrane $\left(\frac{kg}{m}\right)$, $T_o$ is Tension on the membrane $\left(\frac{N}{m}\right)$, $t$ is time (s), $w$ is transverse displacement of the membrane in z-axis and $r$ & $\theta$ are polar coordinates of the membrane.

In solving the equation (2.15) above, the equation is transformed using variable separable method into three equations representing time, radial and azimuthal coordinates independently.

$$w(r, \theta, t) = R(r)\theta(\theta)\kappa(t) \tag{2.17}$$

This leads to three set of second order ordinary differential equations[2].

[1] Membrane Assumptions;It is pertinent to note that a membrane does not account for flexure, thus no bending is accounted for

[2] The third equation is due to the geometry of the membrane, that is a circular membrane, the equations for a rectangular membrane or plate will yield different results

$$\frac{d^2\kappa}{dt^2} + \omega^2\kappa(t) = 0 \tag{2.18}$$

$$\frac{d^2\theta}{d\theta^2} + p^2\theta = 0 \tag{2.19}$$

$$\frac{d^2R(r)}{dr^2} + \frac{1}{r}\frac{dR(r)}{dr} + \left(\pm\lambda^2 - \frac{p^2}{r^2}\right)R(r) = 0 \tag{2.20}$$

Where $\omega$ is natural frequency of the membrane ($\frac{rad}{s}$) , $p$ is arbitrary constant of variable for azimuth representing a periodic frequency and $\lambda = \left(\frac{m}{T_o}\right)^{1/2}\omega$ .

The solutions of these equations (2.21),( 2.22) and (2.23) are as follows

$$T(t) = E\cos(\omega t) + F\sin(\omega t) \tag{2.21}$$

$$\theta(\theta) = G\cos(p\theta) + H_{m_m}\sin(p\theta) \tag{2.22}$$

$$R(r) = I_nJ_n(\lambda r) + L_nJ_n(i\lambda r) + M_nY_n(\lambda r) + N_nY_n(i\lambda r) \tag{2.23}$$

For continuous displacement of the membrane, $\theta(\theta) = 2\pi$, $p$=$n$=1,2,3,4... must be periodic. It is note worthy that from equation (2.20), the periodic displacement of the membrane suggests the roots are complex numbers. These complex numbers are responsible for the order of the Bessel function produced in equation (2.23). The Bessel functions[3] for integers $p$ are known as cylinder functions or cylindrical harmonics because they appear in the solution to Laplace equation in cylindrical coordinates.

E, F, G, $H_{m_m}$, I, L, M, N represents amplitudes and they depend on the initial and boundary conditions.

Where $J_n(\lambda r)$ is Bessel function of the first kind, $n$ is order of the Bessel function and $Y_n(\lambda r)$ is Bessel function of the second kind.

It can be seen from equation (2.23) that the solution to the radial differential equation is a linear combination of Bessel functions of order n. This is simply due to the geometry of the membrane.

The Bessel function of the second kind gives a logarithmic singularity at zero argument, thus is infinite for zero argument, it is important to note that if there is a hole at the center of membrane, for example an annular membrane, the Bessel function of the second kind comes to play in the radial equation Rosenheinrich [16]. In this study, all constant representing Bessel function of the second kind becomes zero since displacement is a finite value. The constant $L_n$ is zero because membrane is being considered [4].

Considering only the time independence of the solution and combining the constants, the displacement of the membrane is given as

$$w(r,\theta) = Q_nJ_n(\lambda r)\cos(n\theta) \tag{2.24}$$

The interest is mainly on the fixed edges of the membrane as it focuses on the experimental set-up by Rizos [1]. The boundary condition as highlighted is easier to reproduce and the experiment was conducted to understand the fluid-structure interaction having one of its aims to have a simple set-up.

[3] Bessel function arises when finding separate solutions to Laplace equation and wave equation in cylindrical or spherical coordinate

[4] This is not the case for a circular plate as the boundary conditions for a membrane eliminates the constant $L_n$

### 2.3.1. FIXED EDGE

Looking at equation (2.15), the boundary condition for a circular fixed membrane with radius, **a**, is

$$w(a,0) = 0 \quad |_{r=a} \tag{2.25}$$

$$w(a,\theta) = Q_n J_n(\lambda a)\cos(n\theta) \tag{2.26}$$

$$J_n(\lambda a) = 0 \tag{2.27}$$

Equation (2.27) gives the frequency equation or characteristics equation of the fixed circular edge in tension, its roots are the natural frequencies of the circular membrane.

In the understanding of the dynamics of a vibrating circular membrane, the membrane is categorized into imaginary[5] orderly spaced diameters $n$ which represents the order of the equations and concentric nodal circles $m$ representing the numerical rank of the root. These two factors largely determines the behaviour of the vibration pattern of the membrane at a distinct frequency. It should be mentioned that when $n$=0, it simply means the membrane exhibits axisymmetric modes and when $n \neq 0$, the membrane exhibits unsymmetric or asymmetric modes[6]. Thus, if $n = 3$ and $m = 3$, it simply means it has a third root and third order which yields the nodal pattern of three nodal circle lines and three nodal diameters respectively.

### 2.3.2. EQUATION OF NODAL DIAMETERS

The dynamics of a vibrating circular membrane depends on equally spaced diameters which it can only be noticed when the membrane is excited at a certain frequency.

$$w_{m,n}(r,\theta) = \left(E_n J_n(\lambda_{m,n} r)\right)\left(G_n \cos(n\theta) + H_n \sin(n\theta)\right) \tag{2.28}$$

The Nodal diameters depends on $n$.

$$w_n(n\theta) = G_n\left(\cos(n\theta) + H_n \sin(n\theta)\right) \tag{2.29}$$

$$w_n(n\theta) = S_n \cos(n\theta - \alpha) \tag{2.30}$$

$$S_n = R_n\sqrt{G_n^2 + H_n^2} \tag{2.31}$$

$$\alpha = \arctan\left(\frac{H_n}{G_n}\right) \tag{2.32}$$

For a specific $\lambda$ and $r$, equation (2.29) can be written as equation (2.30) and equation (2.30) can be rewritten as equation (2.31) where $R_n$ is a constant representing the first term in bracket of equation (2.28).

Equation (2.30) must be zero. Thus, $w = 0$, then $(n\theta - \alpha) = S\left(\frac{\pi}{2}\right)$ where $S = 1,3,5,\ldots$

### 2.3.3. EQUATION OF NODAL CIRCLES

The second parameter in the dynamics of a circular membrane is the nodal circle, it can visualized when the membrane is excited at a particular frequency and it is dependent on radius of the membrane[7].

[5] It is imaginary because it cannot be seen with the naked eyes, but can be noticed when the membrane is excited at a distinct frequency

[6] The axisymmetric mode simply means that the geometry of the membrane is unaltered and asymmetric means the geometry of the membrane is unaltered by diameters.

[7] The nodal circles and diameter depends solely on the mode shapes, these properties of the circular membrane, when excited at a particular frequency, are responsible for the mode shapes

$$w_{m,n}(r) = I_n J_n\left(\lambda_{m,n} r\right) \tag{2.33}$$

Finding the radii, $w_{m,n}(r) = 0$ ; thus

$$I_n J_n(\lambda r) = 0 \tag{2.34}$$

The non-trival solution is of common interest in understanding problems related to dynamics, hence, the radius of the concentric circles depends on the natural frequencies.

The deflection of the circular membrane can be defined as

$$w(r,\theta,t) = V\left(J_n \frac{\lambda_{m,n} r}{a}\right)\cos(n\theta)\cos(\omega t + \phi) \tag{2.35}$$

The first term is the Bessel function in equation (2.35) and it is responsible for the vibration patterns of a fixed circular membrane in figure 2.3 below. For clearer visualization (this is explained in detail in the next chapter). The figure 2.3 is used to further elaborate on the nodal circles and diameters. [8]

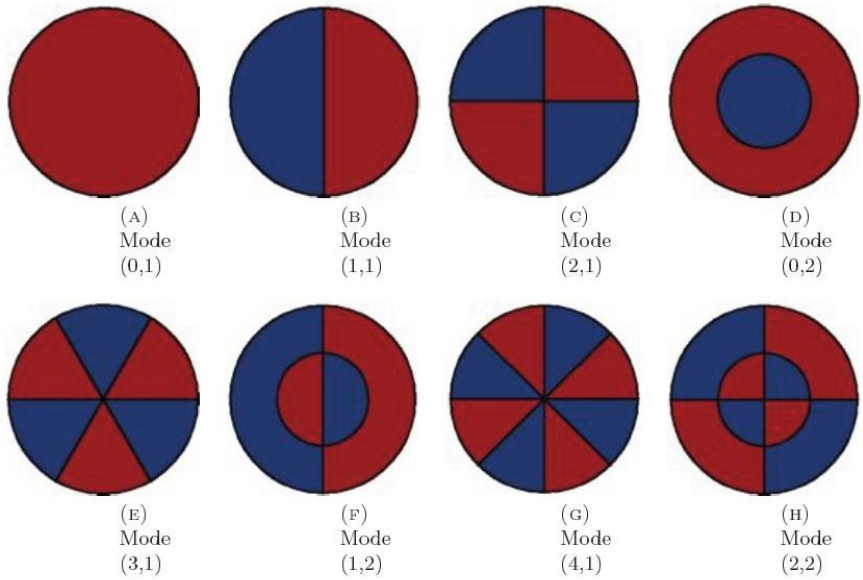


Figure 2.3: Vibration modes of the circular membrane in nodal circles and nodal diameter patterns *In vacuo* [1]

[8] A better representation of the vibration modes are given in the next chapter.

Figure 2.3 above represents the vibration pattern of eight distinct natural frequencies of a fixed circular membrane. It is very important to understand that the vibration mode of a vibrating circular membrane is a function of two modes namely **cosine** and **sine modes**. In equation (2.29) the cosine, sine function or a combination of both can be used to define the nodal diameter and the physical meaning mainly due to the isotropic property [9] of the circular membrane. The origin of the membrane is arbitrary and there can be changed in the rotational direction of the circular membrane that causes *modal degeneracy* in only the asymmetric modes i.e. when $n \neq 0$. This is best seen in figure 2.3 and from equation (2.28), looking at the Mode $(1,1)$, when cosine is 0, at $\frac{\pi}{2}$ , sine is 1 at $\frac{\pi}{2}$, thus you see the nodal diameter appears, and this nodal diameter can be rotated arbitrarily since the origin of the membrane is arbitrary. This simply means that at a distinct frequency, there are two behaviours in the mode shapes due to the cosine and sine functions. The red and blue semicircles clearly shows that at a certain frequency when $\frac{\pi}{2}$ exists, cosine is 0 and sine function is 1 from equation (2.28). This is not the case for all axisymmetric modes, there is rather a creation of the nodal circle as seen in equation (2.35).

## 2.4. DYNAMIC ANALYSIS OF COUPLED FLUID-STRUCTURE INTERACTION 2-D

The problem uses a rectangular container of length **b** with and an elastic string at the bottom and filled with fluid of height **h**. The string deflects as fluid is poured into the container and the exciting force on the strings comes from the pressure of the fluid as shown in the figure 2.4 below.

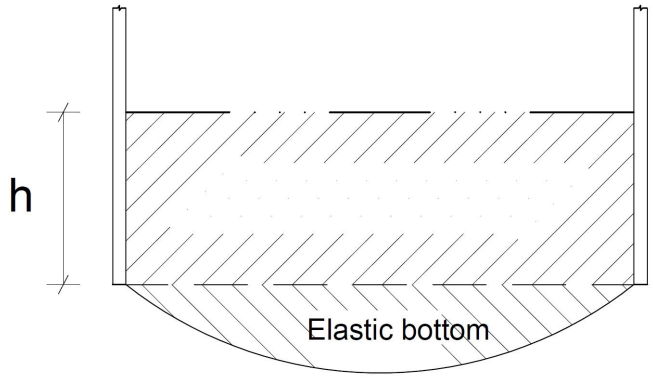


Figure 2.4: Description of the FSI in 2-D case using a string

[9] Isotropy of an object simply means an object having physical property which has the same value when measured from different direction.

The fluid under consideration is assumed to be incompressible, irrotational and non viscous. Linear theory is also assumed. The velocity of the fluid can be represented as the gradient of a velocity potential $\phi$. Hence, the fluid obeys the Laplace equation (2.36).

$$\frac{\partial^2 \phi}{\partial x^2} + \frac{\partial^2 \phi}{\partial z^2} = 0 \tag{2.36}$$

The boundary region to be satisfied are as follows

$$0 \leq x \leq b \quad \& \quad 0 \leq z \leq h \tag{2.37}$$

where $b$ is the length of the rectangular container and $h$ is the height of the fluid column.
The boundary conditions for side walls are

$$\frac{\partial \phi}{\partial x} = 0 \quad \Big|_{x=0 \leq x \leq b} \tag{2.38}$$

$$\frac{\partial \phi}{\partial z} = 0 \quad \Big|_{z=0 \leq z \leq h} \tag{2.39}$$

The free surface dynamic (pressure is constant around the surface) and kinematic condition of the fluid is obtained from the Cauchy-Poisson relationship of $\phi = \eta$. Where, $\eta$ is the surface elevation of the free surface. The fluid particle velocity is equal to the normal velocity of the free surface. The combination of both kinematic and dynamic free surface condition leads to

$$\frac{\partial^2 \phi}{\partial t^2} + g\frac{\partial \phi}{\partial z} = 0 \quad \Big|_{z=h} \tag{2.40}$$

Where $h$ = height of the fluid column.
The loading of the membrane due to the fluid pressures is given by

$$P = -\rho \frac{\partial \phi}{\partial t} \quad \Big|_{z=0} \tag{2.41}$$

Since the bottom of the container is considered to be elastic, the motion can be described as an elastic string given by

$$T\frac{\partial^2 w}{\partial x^2} - m_s \frac{\partial^2 w}{\partial^2 t} = P \tag{2.42}$$

Positive pressure acts on the membrane in a direction opposite to that of positive deflection. Equation (2.43) is a condition where the deflection of the membrane is zero at the edges since it is a fixed boundary condition

$$w = 0 \quad |_{x=0,b} \quad z=0,h \tag{2.43}$$

Particles of the fluid in contact with the membrane and the membrane itself must move with the same velocity. This condition is the so called cavitation or compatibility condition of the fluid at the bottom.

$$\frac{\partial w}{\partial t} = \frac{\partial \phi}{\partial z} \quad \Big|_{z=0} \tag{2.44}$$

### 2.4.1. FLUID DESCRIPTION

The velocity potential of the fluid is given by

$$\phi(x,z,t) = \sum_{d=0}^{\infty} A_d e^{i\omega_c t} \cos\frac{d\pi r}{b}\left(\cosh\frac{d\pi z}{b} + \left(\frac{\omega_c^2 \tanh\frac{d\pi h}{b} - \frac{g\pi d}{b}}{\omega_s^2 - \omega_c^2}\right)\left(\sinh\frac{d\pi z}{b}\right)\right) \tag{2.45}$$

where

$$\omega_s^2 = \frac{g\pi d}{b}\tanh\left(\frac{\pi d h}{b}\right) \tag{2.46}$$

and $k = \frac{d\pi}{b}$ is the wave number and $A_d$ is amplitude of the oscillation, $\omega_s$ is the natural frequency of the liquid in a completely rigid container. $\omega_c$ is the undetermined coupled frequencies of the system. The solution must satisfy the boundary conditions of equation (2.43). Let the deflection of the string be given as

$$w = \sum_{d=0}^{\infty} W_d(t)\sin\frac{d\pi x}{b} \tag{2.47}$$

The kinetic ($X$) and potential ($Y$) energy used in the loading (pressure on the string from the fluid) of the string is given by

$$X = \int_0^b \frac{1}{2v}\left(W_d^2 \sin\frac{d\pi x}{b}\right)^2 dx \tag{2.48}$$

$$Y = \int_0^b \frac{1}{2v}\left(W_d^2\frac{1}{2} - \frac{1}{2}\cos 2x\right)dx \tag{2.49}$$

$$X = \frac{1}{4v} b \sum_{d=0}^{\infty} W_d^2 \tag{2.50}$$

$$Y = \frac{T}{2}\int_0^b \left(\frac{\partial w}{\partial x}\right)^2 dx \tag{2.51}$$

$$Y = \frac{T}{2} W_d(t) \int_0^b \left(\frac{d\pi}{b}\right) cos\left(\frac{d\pi x}{b}\right)^2 dx \tag{2.52}$$

$$Y = W_d(t)\frac{T}{2}\frac{d^2\pi^2}{b^2}\Big|_{z=0}^{z=b} \tag{2.53}$$

$$Y = \sum_{d=0}^{\infty} W_d^2(t)\frac{T}{4}\frac{d^2\pi^2}{b} \tag{2.54}$$

Where $T$ is the tension of the string and $v$ is the representation of mass per unit area. From the principles of virtual work,

$$\delta W = \int_0^b P(x,t)\sum_{d=0}^{\infty}\delta W_{de}\sin\left(\frac{d\pi x}{b}\right)dx \tag{2.55}$$

where $P(x,t)$ is the load function representing pressure exciting force of the fluid on the string and introducing equation (2.41) and equation (2.46) yields the Lagrange equation is given by

$$\ddot{W}_d + \left(\omega_d^2 - \frac{\rho g}{\upsilon}\right) W_d = \frac{2i\rho\omega_c}{\upsilon\pi} \sum_{k=0}^{\infty} e^{i\omega_c t} \int_0^b \sum_{d=0}^{\infty} A_d \cos\left(\frac{d\pi x}{b}\right) \sum_{d=0}^{\infty} \sin\left(\frac{d\pi x}{b}\right) dx \tag{2.56}$$

Considering the Fourier-sine series approximations for

$$\cos\left(\frac{k\pi x}{b}\right) = \sum_{d=0}^{\infty} \alpha^{(k)} \sin\left(\frac{d\pi x}{b}\right) \tag{2.57}$$

$$\alpha^{(k)} = \frac{2}{\pi} \frac{d[1-(-1)^{d+k}]}{(d^2-k^2)} \tag{2.58}$$

$$\alpha_k^{(k)} = 0 \tag{2.59}$$

where the values of $k = 0$ and other values $d + k$ is an odd number. Combining equation (2.42) , (2.43), (2.44) and (2.45) yields the differential equation and

$$W_d = B_d e^{i\omega_c t} \tag{2.60}$$

Thus this yields

$$B_d(-\omega_c^2 + \omega_d^2 - \frac{\rho g}{\upsilon}) - \frac{2i\rho\omega_c}{\upsilon\pi} \sum_{k=0}^{\infty} e^{i\omega_c t} A_d \frac{d[1-(-1)^{d+k}]}{(d^2-k^2)} = 0 \tag{2.61}$$

Now applying equation (2.44)

$$\omega_c i B_d = \sum_{k=0}^{\infty} A_k \frac{d\pi}{b} \frac{2}{\pi} \frac{d[1-(-1)^{d+k}]}{(d^2-k^2)} \left(\frac{\omega_c^2 \tanh(\frac{k\pi h}{b}) - \frac{g\pi k}{b}}{\omega_{s_{(k)}}^2 - \omega_c^2}\right) (-\omega_c^2 + \omega_{d_{(d)}}^2 - \frac{\rho g}{\upsilon}) \tag{2.62}$$

These leads to frequency equation or characteristic equation whose coefficient determinant yields the desired coupled frequencies.

$$\sum_{k=0}^{\infty} A_k \frac{d[1-(-1)^{d+k}]}{(d^2-k^2)} \left(\frac{\rho\omega_c^2}{\upsilon} + (\omega_c^2 - \omega_{d_{(d)}}^2 - \frac{\rho g}{\upsilon})\right) \frac{k\pi}{b} \left(\frac{\omega_c^2 \tanh(\frac{k\pi h}{b}) - \frac{g\pi k}{b}}{\omega_{s_{(k)}}^2 - \omega_c^2}\right) = 0 \tag{2.63}$$

## 2.5. DYNAMIC ANALYSIS OF COUPLED FLUID-STRUCTURE INTERACTION 3-D

The section is studied in two parts, when the membrane is situated at the bottom of the smaller cylinder and when the membrane is situated at the top of the bigger cylinder without the smaller cylinder. This is to help understand how the dynamics of the fluid-structure interaction works with respect to the position of the membrane.

### 2.5.1. MEMBRANE SITUATED AT THE BOTTOM OF CYLINDER

The dynamics of the coupled fluid-structure interaction is divided into two parts from Rizos [1], wherein two cylinders filled with fluid to the same level, although, the smaller cylinder is partly submerged inside the bigger cylinder and is driven harmonically by a motor. The bottom of the smaller cylinder is a flexible membrane. The dynamics of the coupled fluid-structure interaction discussed in this section captures the smaller cylinder with a flexible bottom and rigid walls as shown in figure 2.5 below.

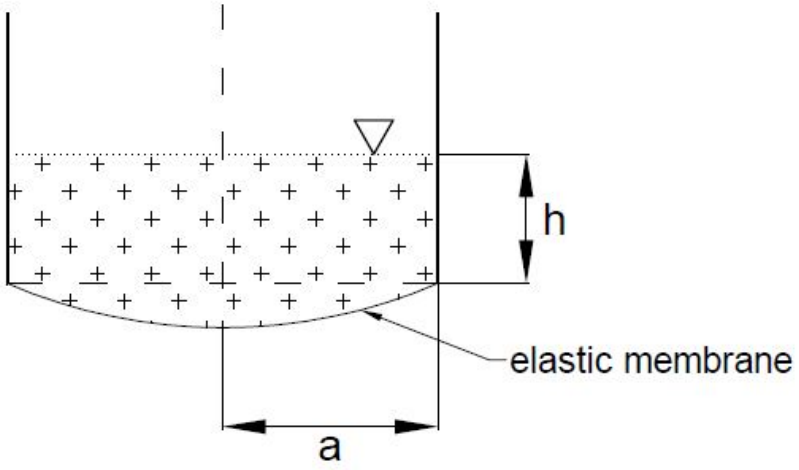


Figure 2.5: Illustration of the coupling phenomenon with membrane located at the bottom of the cylinder in 3-D case

It must be said that the fluid in consideration is water, thus, the assumption made for the analytical solutions are: the fluid is assumed to be non- viscous, incompressible and irrotational. The assumption of the linear theory is used, thus, the harmonic displacements, velocities and accelerations of fluid particles will have a linear relationship with the wave surface elevation. According to Rizos [1], the exciting motor must possess a harmonic motion also. The velocity potential $\phi(r,\theta,z,t)$ must satisfy the so called governing equations which are continuity equation, bottom boundary conditions, free surface dynamic and kinematic conditions.

Laplace or continuity condition for a cylindrical coordinate is given as

$$\frac{\partial u}{\partial r}+\frac{u}{r}+\frac{\partial v}{\partial \theta}+\frac{\partial w}{\partial z}=0 \tag{2.64}$$

Where

$$u=\frac{\partial \phi}{\partial r} \quad ,v=\frac{1}{r}\frac{\partial \phi}{\partial \theta} \quad ,w=\frac{\partial \phi}{\partial z} \tag{2.65}$$

u, v, and w are the velocities in the direction of the cylindrical axis. Combining equation (2.64) and equation (2.65) gives

$$\frac{\partial^2 \phi}{\partial r^2}+\frac{1}{r}\frac{\partial \phi}{\partial r}+\frac{1}{r^2}\frac{\partial^2 \phi}{\partial \theta^2}+\frac{\partial^2 \phi}{\partial z^2}=0 \tag{2.66}$$

The combination of dynamic and kinematic free surface condition states that pressure is constant across the surface and particles on the free surface move with a velocity of the free surface. This yields equation (2.67)

$$\frac{\partial^2 \phi}{\partial t^2}+g\frac{\partial \phi}{\partial z}=0 \quad \Big|_{z=h} \tag{2.67}$$

Where $h$ = height of the fluid column of the small cylinder.

Other equations include velocity potential at walls equals to zero equations (2.68) and the dynamic boundary condition due to fluid pressure at the bottom yields equation (2.69).

$$\frac{\partial \phi}{\partial r} = 0 \quad \Big|_{r=a} \tag{2.68}$$

$$P = -\rho \frac{\partial \phi}{\partial t} \quad \Big|_{z=0} \tag{2.69}$$

From equation (2.15), the coupling conditions are as follows in the equations (2.70) and equation (2.71).

$$T_o \nabla^2 w - m_m \frac{\partial^2 w}{\partial^2 t} = P \tag{2.70}$$

Positive pressure acts on the membrane in a direction opposite to that of positive deflection. Equation (2.71) is a condition where the deflection of the membrane is zero at the edges since it is a fixed boundary condition

$$w = 0 \quad |_{r=a} \tag{2.71}$$

Particles of the liquid in contact with the membrane and the membrane itself must move with the same velocity. This condition is the so called cavitation or compatibility condition of the fluid at the bottom.

$$\frac{\partial w}{\partial t} = \frac{\partial \phi}{\partial z} \quad \Big|_{z=0} \tag{2.72}$$

For this condition, the non-linear terms are neglected and liquid velocity is evaluated at the undisturbed position of the membrane. Having defined the above equations, the solution to this coupling problem depends on the representation of the velocity potential of the fluid. Due to geometry and nature of the problem, it is not uncommon that fluid takes the shape(volume) of its container when all external excitation is absent. The vibration modes of a fixed circular membrane *In Vacuo* exhibits a Bessel function thus, the velocity potential is also represented by a Bessel function in equation (2.73). The geometry of the membrane is a circle and it is common knowledge that a circle has infinite number of symmetric lines and can as well be considered to be asymmetric depending on the manner the lines of symmetry are drawn. For the benefit of ease in understanding, the circular membrane was separated into axisymmetric and asymmetric cases.

### AXISYMMETRIC CASE

This is the case when all nodal diameter are considered absent; the solutions to this problem are as follows and only the nodal circle is considered, thus $n = 0$ and $m \neq 0$. The velocity potential is defined as follows:

$$\phi_n = A_n J_0(k_n r)(e^{-k_n z} + B_n e^{k_n z}) e^{i\omega_c t} \quad \Big|_{k_n \neq 0} \tag{2.73}$$

Where, $A_n$, $B_n$ and $k_n$ are wave amplitudes and wave number respectively. $\omega_c$ is the unknown coupled frequency of the membrane and the fluid. The total velocity potential is the sum of all velocity potentials around the cylinder from $\phi_n$ ; $n = 0...\infty$. This comes from the so called additive property of angular momentum.

The geometry of the membrane is a circle and the wave particles tend to rotate relative to the centre of the membrane. Combining these two features, the velocity potential is defined as specific relative angular momentum and conservation is of importance – angular momentum is a conserved quantity.

The solution to equation (2.73) when $k_n$ equals zero and $r = 0$ is the velocity potential when the nodal circle is zero gives the equation (2.74) which is a regular solution and fulfils equation (2.66).

$$\phi_0 = A_0(Z + B_0)e^{i\omega_c t} \quad \Big|_{k_n=0} \tag{2.74}$$

Applying the free surface conditions in equations (2.67), (2.73) and (2.74) yields;

$$B_n = \frac{(gk_n + \omega_c^2)e^{-k_n h}}{(gk_n - \omega_c^2)e^{k_n h}} \quad \Big|_{k_n \neq 0, z=h} \tag{2.75}$$

$$B_0 = \frac{g - h\omega_c^2}{\omega_c^2} \quad \Big|_{k_n=0, z=h} \tag{2.76}$$

Applying equation (2.68) to equation (2.73) yields

$$J_1(k_n a) = 0 \quad |_{r=a} \tag{2.77}$$

The roots (**zero-crossings**) of equation (2.77) gives the value of $k_n$ in figure 2.6 below. To solve equation (2.70), an expression for equation (2.69) when $k_n$ equals zero and non-zero is applied to equation (2.73) which yields

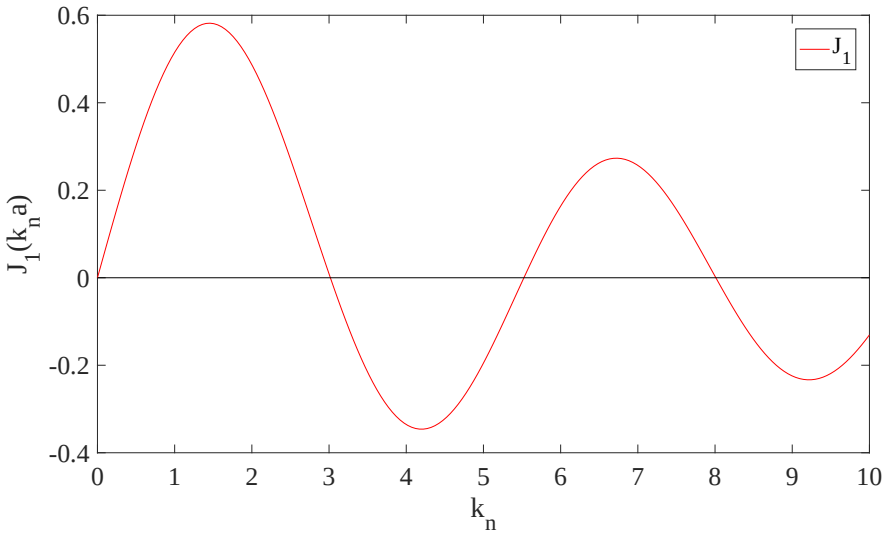


Figure 2.6: The wave number $k_n$ plot as a function of the Bessel function

From equation (2.69), it yields equations (2.78) and (2.79)

$$-\rho i\omega_c e^{i\omega_c t} A_n J_0(k_n r)(B_n+1) = P_n \quad \Big|_{k_n\neq 0} \tag{2.78}$$

$$-\rho i\omega_c e^{i\omega_c t} A_0 B_0 = P_0 \quad \Big|_{k_n=0} \tag{2.79}$$

Let the membrane deflection take the form

$$w = W_n(r) e^{i\omega_c t} \quad \Big|_{n\neq 0} \tag{2.80}$$

$$w = W_0(r) e^{i\omega_c t} \quad \Big|_{n=0} \tag{2.81}$$

In solving equation (2.70),substitute equations (2.80) and (2.81) to give

$$\frac{d^2 W_n}{dr^2} + \frac{1}{r}\frac{dW_n}{dr} + \mu^2 W_n = \frac{-\rho i\omega_c}{T_0} A_n(1+B_n) J_0(k_n r) \tag{2.82}$$

The solution to equation (2.82) yields

$$W_n = \gamma\prime_n \left( J_0(k_n r) - \frac{J_0(\mu r) J_0(k_n a)}{J_0(\mu a)} \right) \tag{2.83}$$

$$\gamma\prime_n = \frac{-\rho i\omega_c A_n(1+B_n)}{T_0(\mu^2 - k_n^2)} \tag{2.84}$$

$$\mu^2 = \frac{m_m \omega_c^2}{T_0} \tag{2.85}$$

Similarly, when $k_n$ equals zero

$$\frac{d^2 W_0}{dr^2} + \frac{1}{r}\frac{dW_0}{dr} + \mu^2 W_0 = \frac{-\rho i\omega_c}{T_0} A_0 B_0 \tag{2.86}$$

$$W_0 = \gamma\prime_0 \left( 1 - \frac{J_0(\mu r)}{J_0(\mu a)} \right) \tag{2.87}$$

$$\gamma\prime_0 = \frac{-\rho i\omega_c A_0 B_0}{T_0(\mu^2)} \tag{2.88}$$

Substituting equations (2.77), (2.78) and (2.79) into equations (2.80) and (2.81) respectively and finally applying the cavitation condition in equation (2.72) yields;

$$i\omega_c \gamma\prime_0 \left( 1 - \frac{J_0(\mu r)}{J_0(\mu a)} \right) e^{i\omega_c t} + \sum_{n=1}^{\infty} i\omega_c \gamma_n \left( J_0(k_n r) - \frac{J_0(k_n a)}{J_0(\mu a)} J_0(\mu r) \right) e^{i\omega_c t}$$
$$= A_0 e^{i\omega_c t} + \sum_{n=1}^{\infty} k_n A_n (B_n - 1) J_0(k_n r) e^{i\omega_c t} \tag{2.89}$$

By comparison of equation (2.89), the coefficients of $A_0$ and $A_n$ gives the values of the coupled natural frequency. Expanding $J_0(\mu r)$ into $J_0(k_n r)$ using Dini series also known as Fourier-Bessel series [17] and equating the coefficient terms on both sides leads to equation (2.90).

$$J_0(\mu r) = \frac{2}{a\mu} J_1(\mu a) + \sum_{m=1}^{\infty} \frac{2}{a(\mu^2 - k_m^2)} \frac{J_1(\mu a)}{J_0(k_n)} J_0(k_m r) \tag{2.90}$$

Substituting equation (2.90) into equation (2.89), the solution of the constants $A_n$ equation (2.91) yields

$$i\omega_c\gamma_{0\prime} - i\omega_c\gamma_{0\prime}\frac{2J_1(\mu a)}{a\mu J_0(\mu a)} - i\omega_c\gamma_{0\prime}\frac{2\mu J_1(\mu a)}{aJ_0(\mu a)}\sum_{m=1}^{\infty}\frac{1}{(\mu^2-k_m^2)}\frac{J_0(k_m r)}{J_0(k_m a)} + \sum_{n=1}^{\infty} i\omega_c\gamma_{n\prime}J_0(k_n r) - \sum_{n=1}^{\infty} i\omega_c\gamma_{n\prime}\frac{J_0(k_n a)}{J_0(\mu a)}\frac{2J_1(\mu a)}{a\mu} - \sum_{n=1}^{\infty} i\omega_c\gamma_{n\prime}\frac{J_0(k_n a)}{J_0(\mu a)}\sum_{m=1}^{\infty}\frac{2\mu J_1(\mu a)J_0(k_m r)}{a(\mu^2-k_m^2)J_0(k_m a} = A_0 + \sum_{n=1}^{\infty} k_n A_n\,(B_n-1)\,J_0(k_n r) \quad (2.91)$$

In obtaining the coefficients of $A_n$, by comparison of equation (2.91),

$$i\omega_c\gamma_{0\prime} - i\omega_c\gamma_{0\prime}\left(\frac{2J_1(\mu a)}{a\mu J_0(\mu a)}\right) = A_0 \quad (2.92)$$

Thus coefficients of $A_0$ is obtained by substituting equation (2.88) into equation (2.92)

$$i\omega_c\left(\frac{-\rho i\omega_c A_0 B_0}{T_0\mu^2}\right) - i\omega_c\left(\frac{\rho i\omega_c A_0 B_0}{T_0\mu^2}\right)\left(\frac{2J_1(\mu a)}{a\mu J_0(\mu a)}\right) = A_0 \quad (2.93)$$

Yields

$$\left(\frac{\rho\omega_c^2 A_0 B_0}{T_0\mu^2}\right) - \left(\frac{\rho\omega_c^2 A_0 B_0 2J_1(\mu a)}{T_0\mu^3 a J_0(\mu a)}\right) - A_0 = 0 \quad (2.94)$$

Simplifying equation (2.94) by dividing through by $A_0$ and making $J_0(\mu a)$=1 and $\frac{J_1(\mu a)}{\mu a} = 0.5$ because of the asymptote values are easier to approximate.

$$\alpha_{11} = \left(\frac{\rho\omega_c^2 B_0}{T_0\mu^2}\right) - \left(\frac{\rho\omega_c^2 B_0 2J_1(\mu a)}{T_0\mu^3 a J_0(\mu a)}\right) - 1 \quad (2.95)$$

Similarly, from equation (2.91) yields equation (2.96)

$$-i\omega_c\left(\frac{-\rho i\omega_c A_n(1+B_n)}{T_0(\mu^2-k_n^2)}\right)\left(\frac{J_0(k_n a)}{J_0(\mu a)}\right)\left(\frac{2J_1(\mu a}{a\mu}\right) = 0 \quad (2.96)$$

The coefficient of $\alpha_{12}$ yields equation (2.97) when $n$=1

$$\alpha_{12} = \left(\frac{-2\rho\omega_c^2(1+B_1)J_0(k_1 a)J_1(\mu a)}{T_0 a\mu(\mu^2-k_1^2)J_0(\mu a)}\right) \quad (2.97)$$

When equation (2.96) has $n$=2

$$\alpha_{13} = \left(\frac{-2\rho\omega_c^2(1+B_2)J_0(k_2 a)J_1(\mu a)}{T_0 a\mu(\mu^2-k_2^2)J_0(\mu a)}\right) \quad (2.98)$$

From equation (2.91) comparing coefficients yields equation (2.99)

$$i\omega_c\left(\frac{-\rho i\omega_c A_0 B_0}{T_0\mu^2}\right)\left(\frac{-2\mu J_1(\mu a)}{a(J_0\mu a)}\right)\sum_{m=1}^{\infty}\left(\frac{1}{(\mu^2-k_m^2)}\frac{J_0(k_m r)}{J_0(k_m a)}\right) = 0 \quad (2.99)$$

when n = 1 and n =2 yields

$$\alpha_{21} = \frac{-2\rho\omega_c^2 B_0 J_1(\mu a)}{T_0 \mu a J_0(\mu a)(\mu^2 - k_1^2) J_0(k_1 a)} \tag{2.100}$$

$$\alpha_{31} = \frac{-2\rho\omega_c^2 B_0 J_1(\mu a)}{T_0 \mu a J_0(\mu a)(\mu^2 - k_2^2) J_0(k_2 a)} \tag{2.101}$$

Following the same procedure of comparing the coefficients of $A_0$ and $A_n$

$$\alpha_{22} = \frac{-2\rho\mu\omega_c^2(1+B_1)J_1(\mu a)}{T_0 \mu a((\mu^2 - k_1^2)^2)} + \frac{\rho\omega_c^2(1+B_1)}{T_0(\mu^2 - k_1^2)} - k_1(B_1 - 1) \tag{2.102}$$

$$\alpha_{33} = \frac{-2\rho\mu\omega_c^2(1+B_2)J_1(\mu a)}{T_0 \mu a((\mu^2 - k_2^2)^2)} + \frac{\rho\omega_c^2(1+B_2)}{T_0(\mu^2 - k_2^2)} - k_1(B_2 - 1) \tag{2.103}$$

Finally,

$$\alpha_{23} = \frac{-2\mu\rho\omega_c^2(1+B_2)J_0(k_2 a)J_1(\mu a)}{T_0 \mu a(\mu^2 - k_1^2)J_0(k_1 a)(\mu^2 - k_2^2)J_0(\mu a)} \tag{2.104}$$

$$\alpha_{32} = \frac{-2\mu\rho\omega_c^2(1+B_1)J_0(k_1 a)J_1(\mu a)}{T_0 \mu a(\mu^2 - k_1^2)J_0(k_2 a)(\mu^2 - k_2^2)J_0(\mu a)} \tag{2.105}$$

The determinant of the $A$ matrix below gives the required coupled frequency or frequency determinant obtained by solving the set of simultaneous equation(2.91).

$$A = \begin{vmatrix} \alpha_{11} & \alpha_{12} & \alpha_{13} & \dots \\ \alpha_{21} & \alpha_{22} & \alpha_{23} & \dots \\ \alpha_{31} & \alpha_{32} & \alpha_{33} & \dots \\ \vdots & \vdots & \vdots & \vdots \end{vmatrix}$$

### ASYMMETRIC CASE

This is the case when all nodal circles and nodal diameters are considered, thus $m \neq 0$ and $n \neq 0$. Just like in the axisymmmetric case, the velocity potential is:

$$\phi_{mn} = A_{mn} J_{mn}(k_{mn} r)(e^{-k_{mn} z} + B_{mn} e^{k_{mn} z}) e^{i\omega_c t} \cos(m\theta) \tag{2.106}$$

Applying equation (2.67) to (2.106) to get equation (2.107)

$$B_{mn} = \frac{(g k_{mn} + \omega_c^2) e^{-k_{mn} h}}{(g k_{mn} - \omega_c^2) e^{k_{mn} h}} \tag{2.107}$$

Applying equation (2.68) to equation (2.106) yields equation (2.108)

$$J\prime_n(k_{mn}) = 0 \qquad m = 1, 2, 3, \dots \tag{2.108}$$

The prime stands for the differentiation of Bessel function with respect to the argument. From equation (2.69) the pressure is obtained by

$$P_{mn} = -\rho i \omega_c e^{i\omega_c t} A_{mn} J_m(k_{mn} r)(B_{mn} + 1) \cos(m\theta) \tag{2.109}$$

The membrane deflection from equations (2.70) and (2.71) gives equation (2.110)

$$w = W_{mn}(r)\cos(m\theta)e^{i\omega_c t} \tag{2.110}$$

Substituting equation (2.70) into equations (2.109) and (2.110) yields

$$\frac{d^2W_{mn}}{dr^2} + \frac{1}{r}\frac{dW_{mn}}{dr} + \left(\mu^2 - \frac{m^2}{r^2}\right)W_{mn} = \frac{-\rho i\omega_c A_{mn}J_m(k_{mn}r)(1+B_{mn})}{T_0} \tag{2.111}$$

Solving the differential equation in (2.111) above yields

$$W_{mn} = \gamma\prime_{mn}\left(J_m(k_{mn}r) - \frac{J_m(k_{mn}a)J_m(\mu r)}{J_m(\mu a)}\right) \tag{2.112}$$

$$\gamma\prime_{mn} = \frac{-\rho i\omega_c A_{mn}(1+B_n)}{T_0(\mu^2 - k_{mn}^2)} \quad ;\mu \neq k_{mn} \tag{2.113}$$

$$\mu^2 = \frac{m_m\omega_c^2}{T_0} \tag{2.114}$$

From equation (2.72) the cavitation boundary condition is;

$$\sum_{m=1}^{\infty} i\omega_c\gamma\prime_{mn}\left(J_m(k_{mn}r) - \frac{J_m(k_{mn}r)}{J_m(\mu a)}\right)J_m(\mu r)\,e^{i\omega_c t} = \sum_{n=1}^{\infty} k_{mn}A_{mn}(B_{mn}-1)\,J_m(k_{mn}r)e^{i\omega_c t} \quad m = 1,2,3,\ldots \tag{2.115}$$

Expanding $J_m(\mu r)$ [17] gives ;

$$J_{mn}(\mu r) = \sum_{q=1}^{\infty}\delta_q J_m(k_{mp}r) \tag{2.116}$$

where

$$\delta_q = \frac{2ak_{mq}^2}{(k_{mq}^2a^2 - m^2)((J_m(k_{mq}^2)a))^2(k_{mq}^2 - \mu^2)} \times k_{mq}J_m(\mu a)J_{m+1}(k_{mq}a) - \mu J_m(k_{mq}a)J_{m+1}(\mu a) \tag{2.117}$$

Substituting equations (2.116) and (2.117) into (2.115) yields

$$\sum_{n=1}^{\infty}\gamma_{mn}J_m(k_{mn}r) - \sum_{n=1}^{\infty}\gamma_{mn}\frac{J_m(k_{mn}a)}{J_m(\mu a)}\sum_{q=1}^{\infty}\delta_q J_m(k_{mq}r) = \sum_{n=1}^{\infty}k_{mn}A_{mn}(B_{mn}-1)\,J_m(k_{mn}r) \quad m = 1,2,3,\ldots \quad \text{where} \quad \gamma_{mn} = \gamma\prime_{mn}i\omega_c \tag{2.118}$$

Similarly, by comparing coefficients of equation (2.118) the following elements of the matrix $B$ is obtained.

$$\beta_{11} = \frac{-\rho\omega_c^2(1+B_{m1})J_m(k_{m1a})\delta_1}{T_0(\mu^2-k_{m1}^2)J_m(\mu a)} + \frac{\rho\omega_c^2(1+B_{m1})}{T_0(\mu^2-k_{m1}^2)} - k_{m1}(B_{m1}-1) \tag{2.119}$$

$$\beta_{12} = \frac{-\rho\omega_c^2(1+B_{m2})J_m(k_{m2}a)\delta_1}{T_0(\mu^2-k_{m2}^2)J_m(\mu a)} \tag{2.120}$$

$$\beta_{13} = \frac{-\rho\omega_c^2(1+B_{m3})J_m(k_{m3}a)\delta_1}{T_0(\mu^2-k_{m3}^2)J_m(\mu a)} \tag{2.121}$$

$$\beta_{21} = \frac{-\rho\omega_c^2(1+B_{m1})J_m(k_{m1}a)\delta_2}{T_0(\mu^2-k_{m1}^2)J_m(\mu a)} \tag{2.122}$$

$$\beta_{22} = \frac{-\rho\omega_c^2(1+B_{m2})J_m(k_{m2a})\delta_2}{T_0(\mu^2-k_{m2}^2)J_m(\mu a)} + \frac{\rho\omega_c^2(1+B_{m2})}{T_0(\mu^2-k_{m2}^2)} - k_{m2}(B_{m2}-1) \tag{2.123}$$

$$\beta_{23} = \frac{-\rho\omega_c^2(1+B_{m3})J_m(k_{m3}a)\delta_2}{T_0(\mu^2-k_{m3}^2)J_m(\mu a)} \tag{2.124}$$

$$\beta_{31} = \frac{-\rho\omega_c^2(1+B_{m1})J_m(k_{m1}a)\delta_3}{T_0(\mu^2-k_{m1}^2)J_m(\mu a)} \tag{2.125}$$

$$\beta_{32} = \frac{-\rho\omega_c^2(1+B_{m2})J_m(k_{m2}a)\delta_3}{T_0(\mu^2-k_{m2}^2)J_m(\mu a)} \tag{2.126}$$

$$\beta_{33} = \frac{-\rho\omega_c^2(1+B_{m3}J_m(k_{ma})\delta_3}{T_0(\mu^2-k_{m3}^2)J_m(\mu a)} + \frac{\rho\omega_c^2(1+B_{m3})}{T_0(\mu^2-k_{m3}^2)} - k_{m3}(B_{m3}-1) \tag{2.127}$$

Similarly, the determinant of Matrix $B$ gives the coupled frequency or frequency determinant obtained by solving the set of simultaneous equation obtained from equation (2.118) of the system in the asymmetric case.

$$B = \begin{vmatrix} \beta_{11} & \beta_{12} & \beta_{13} & \dots \\ \beta_{21} & \beta_{22} & \beta_{23} & \dots \\ \beta_{31} & \beta_{32} & \beta_{33} & \dots \\ \vdots & \vdots & \vdots & \vdots \end{vmatrix}$$

### 2.5.2. MEMBRANE SITUATED AT THE TOP OF CYLINDER

In this case, the membrane lies on the free surface of the bigger cylinder with radius **R** and height **H** but not entirely. This is considered because, the free surface effect must be captured. Following the governing equations, the following modifications are made to the membrane at the top as seen in the figure 2.7 below.

Laplace or continuity condition for a cylindrical coordinate is given as

$$\frac{\partial u}{\partial r} + \frac{u}{r} + \frac{\partial v}{\partial \theta} + \frac{\partial w}{\partial z} = 0 \tag{2.128}$$

Where

$$u = \frac{\partial \phi}{\partial r} \quad , v = \frac{1}{r}\frac{\partial \phi}{\partial \theta} \quad , w = \frac{\partial \phi}{\partial z} \tag{2.129}$$

u, v, and w are the velocities in the direction of the cylindrical axis. Combining equation (2.128) and (2.129) gives the Laplace or continuity condition for a cylindrical coordinate.

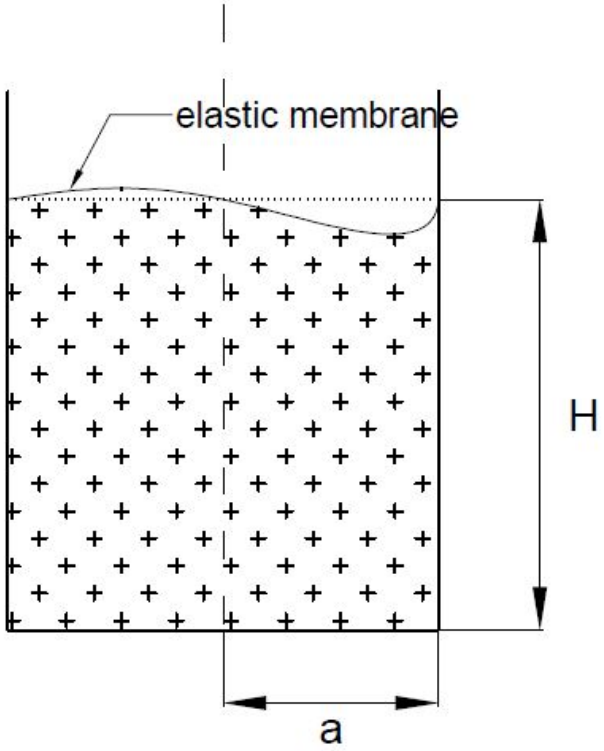


Figure 2.7: Description of the coupling phenomenon with membrane located at the top of the cylinder 3-D case

$$\frac{\partial^2\phi}{\partial r^2}+\frac{1}{r}\frac{\partial\phi}{\partial r}+\frac{1}{r^2}\frac{\partial^2\phi}{\partial\theta^2}+\frac{\partial^2\phi}{\partial z^2}=0 \tag{2.130}$$

The combination of dynamic and kinematic free surface condition yields equation (2.131)

$$\frac{\partial^2\phi}{\partial t^2}+g\frac{\partial\phi}{\partial z}=0 \quad \Big|_{z=H} \quad a\le r\le R \tag{2.131}$$

Where $H$ = height of the fluid column of the small cylinder. [10]

Other equations include velocity potential at walls equals to zero equations (2.132) and the dynamic boundary condition due to fluid pressure at the bottom yields equation (2.133).

$$\frac{\partial\phi}{\partial r}=0 \quad \Big|_{r=R} \tag{2.132}$$

$$P=\rho\frac{\partial\phi}{\partial t} \quad \Big|_{z=H} \tag{2.133}$$

From equation (2.15), the coupling conditions are as follows in the equations (2.134) and equation (2.135).

$$T_o\nabla^2 w-m_m\frac{\partial^2 w}{\partial^2 t}=P \tag{2.134}$$

[10] It should be noted that for the case of the membrane covering located at the top of the cylinder, there is no free-surface boundary condition considered in the analysis.

Positive pressure acts on the membrane in a direction same to that of positive deflection. Equation (2.135) is a condition where the deflection of the membrane is zero at the edges since it is a fixed boundary condition

$$w = 0 \quad |_{r=a} \tag{2.135}$$

Particles of the liquid in contact with the membrane and the membrane itself must move with the same velocity. This condition is the so called cavitation or compatibility condition of the fluid at the bottom.

$$\frac{\partial w}{\partial t} = \frac{\partial \phi}{\partial z} \quad \Big|_{z=H} \quad 0 \le r \le a \tag{2.136}$$

In this particular case, the axisymmetric case is taken into consideration, this is when all nodal diameter are considered absent. The solution to this problem is as follows and only the nodal circle is considered, thus $n = 0$ and $m \neq 0$.

$$\phi_n = A_n J_0\left(k_n \frac{r}{R}\right)\left(e^{-k_n \frac{z}{R}}\right) + B_n\left(e^{k_n \frac{z}{R}}\right) e^{i\omega_c t} \quad \Big|_{k_n \neq 0} \tag{2.137}$$

Where, $A_n$,$B_n$ and $k_n$ are wave amplitudes and wave number respectively. $\omega_c$ is the unknown coupled frequency of the membrane and the fluid.

To solve equation (2.138) when $k_n$ is not zero. The solution to $k_n$ equals zero and $r$=0 is the velocity potential where nodal circles is zero gives the equation (2.138).

$$\phi_0 = A_0\left(\frac{Z}{R} + B_0\right) e^{i\omega_c t} \quad \Big|_{k_n=0} \tag{2.138}$$

Applying the free surface conditions in equations (2.131) and (2.137) and (2.138) yields

$$B_n = \frac{(g\frac{k_n}{R} + \omega_c^2)e^{-k_n \frac{H}{R}}}{(g\frac{k_n}{R} - \omega_c^2)e^{k_n \frac{H}{R}}} \quad \Big|_{k_n \neq 0, z=H} \tag{2.139}$$

$$B_0 = \frac{\frac{g}{R} - \frac{H}{R}\omega_c^2}{\omega_c^2} \quad \Big|_{k_n=0, z=H} \tag{2.140}$$

The boundary condition at the bottom where $z$=0 from equation (2.137)

$$A_0 e^{i\omega_c t} + A_n J_0(k_n r) e^{i\omega_c t} k_n (B_n - 1) = 0 \quad \Big|_{k_n=0, z=0} \tag{2.141}$$

This condition is only satisfied when $B_n = 1$

Applying equation (2.132) to equation (2.137) yields:

$$J_1(k_n a) = 0 \quad |_{r=R} \tag{2.142}$$

The roots of equation (2.142) follow the same values $k_n$ in figure 2.6 above but with different radius since the bigger cylinder has a bigger radius. $k_n$ equals zero and non-zero is applied to equation (2.137) which yields

From equation (2.133), it yields equations (2.143) and (2.144)

$$\rho i\omega_c e^{i\omega_c t} A_n J_0\left(k_n \frac{r}{R}\right)\left(B_n e^{k_n \frac{H}{R}} + e^{-k_n \frac{H}{R}}\right) = P_n \quad \Big|_{k_n \neq 0} \tag{2.143}$$

$$\rho i\omega_c e^{i\omega_c t} A_0\left(\frac{H}{R} + B_0\right) = P_0 \quad \Big|_{k_n=0} \tag{2.144}$$

Let the membrane deflection take the form

$$w = W_n(r)e^{i\omega_c t} \Big|_{n\neq 0} \tag{2.145}$$

$$w = W_0(r)e^{i\omega_c t} \Big|_{n=0} \tag{2.146}$$

In solving equation (2.134),substitute equations (2.145) and (2.146) to give;

$$\frac{d^2W_n}{dr^2} + \frac{1}{r}\frac{dW_n}{dr} + \mu^2 W_n = \frac{\rho i\omega_c}{T_0} A_n \left(e^{-k_n \frac{H}{R}} + B_n e^{k_n \frac{H}{R}}\right) J_0(k_n r) \tag{2.147}$$

The solution to equation (2.147) yields

$$W_n = \delta\imath_n \left(-J_0(k_n \frac{r}{R}) + \frac{J_0(k_n \frac{r}{R}) J_0(\mu r)}{J_0(\mu a)}\right) \tag{2.148}$$

$$\delta\imath_n = \frac{\rho i\omega_c A_n (e^{-k_n \frac{H}{R}} + B_n e^{k_n \frac{H}{R}})}{T_0\mu^2} \tag{2.149}$$

$$\mu^2 = \frac{m\omega_c^2}{T_0} \tag{2.150}$$

Similarly, when $k_n$ equals zero

$$\frac{d^2W_0}{dr^2} + \frac{1}{r}\frac{dW_0}{dr} + \mu^2 W_0 = \frac{\rho i\omega_c}{T_0} A_0 \left(B_0 + \frac{H}{R}\right) \tag{2.151}$$

$$W_0 = \delta\imath_0 \left(1 - \frac{J_0(\mu r)}{J_0(\mu a)}\right) \tag{2.152}$$

$$\delta\imath_0 = \frac{\rho i\omega_c A_0 \left(\frac{H}{R} + B_0\right)}{T_0\mu^2} \tag{2.153}$$

Substituting equations (2.151) , (2.135), (2.147),(2.143) into equations (2.145) and (2.146) respectively and finally applying the cavitation condition in equation (2.136) yields

$$i\omega_c \delta\imath_0 \left(1 - \frac{J_0(\mu r)}{J_0(\mu a)}\right) e^{i\omega_c t} + \sum_{n=1}^{\infty} i\omega_c \delta_n \left(J_0(k_n \frac{r}{R}) - \left(\frac{J_0(k_n \frac{r}{R}) J_0(\mu r)}{J_0(\mu a)}\right) e^{i\omega_c t}\right.$$
$$= A_0 e^{i\omega_c t} + \sum_{n=1}^{\infty} \frac{k_n}{R} A_n \left(B_n e^{k_n \frac{H}{R}} + e^{-k_n \frac{H}{R}}\right) J_0(k_n \frac{r}{R}) e^{i\omega_c t} \tag{2.154}$$

By comparison of equation (2.143), the coefficients of $A_0$ and $A_n$ gives the values of the coupled natural frequency. Expanding $J_0(\mu r)$ into $J_0(k_n r)$ by Fourier-Bessel series [17] and equating the coefficient terms on both sides leads to equation (2.90).

$$J_0(\mu r) = \frac{2}{a\mu} J_1(\mu a) + \sum_{n=1}^{\infty} \frac{2}{a(\mu^2 - k_n^2)} \frac{J_1(\mu a)}{J_0(k_n)} J_0\left(k_m \frac{r}{R}\right) \tag{2.155}$$

Substituting equation (2.155) into equation (2.154), the solution of the constants $A_n$ yields equation (2.156).

$$i\omega_c\delta_0\prime - i\omega_c\delta_0\prime\left(\frac{2J_1(\mu a)}{a\mu J_0(\mu a)}\right) - i\omega_c\delta_0\prime\frac{2\mu J_1(\mu a)}{aJ_0(\mu a)}\sum_{m=1}^{\infty}\frac{1}{(\mu^2-k_m^2)}\frac{J_0(k_m\frac{r}{R})}{J_0(k_m a)} + \sum_{n=1}^{\infty} i\omega_c\delta_n\prime J_0\left(k_n\frac{r}{R}\right)$$
$$- \sum_{n=1}^{\infty} i\omega_c\delta_n\prime\frac{J_0(k_n\frac{r}{R})}{J_0(\mu a)}\left(\frac{2J_1(\mu a)}{a\mu}\right) - \sum_{n=1}^{\infty} i\omega_c\delta_n\prime\frac{J_0(k_n\frac{r}{R})}{J_0(\mu a)}\sum_{m=1}^{\infty}\frac{2\mu J_1(\mu a)J_0(k_m\frac{r}{R})}{a(\mu^2-k_m^2)J_0(k_m a)}$$
$$= A_0 + \sum_{n=1}^{\infty} k_n A_n\left(B_n e^{k_n\frac{H}{R}} + e^{-k_n\frac{H}{R}}\right)J_0\left(k_n\frac{r}{R}\right) \quad (2.156)$$

In obtaining the coefficients of $A_n$, by comparison of equation (2.156)

$$i\omega_c\delta_0\prime - i\omega_c\delta_0\prime\left(\frac{2J_1(\mu a)}{a\mu J_0(\mu a)}\right) = A_0 \quad (2.157)$$

Thus coefficients of $A_0$ is obtained by substituting equation (2.156) into equation (2.171)

$$i\omega_c\left(\frac{\rho i\omega_c A_0(\frac{H}{R}+B_0)}{T_0\mu^2}\right) - i\omega_c\left(\frac{-\rho i\omega_c A_0(\frac{H}{R}+B_0)}{T_0\mu^2}\right)\left(\frac{2J_1(\mu a)}{a\mu J_0(\mu a)}\right) = A_0 \quad (2.158)$$

Yields

$$\left(\frac{\rho\omega_c^2 A_0(\frac{H}{R}+B_0)}{T_0\mu^2}\right) + \left(\frac{\rho\omega_c^2 A_0(\frac{H}{R}+B_0)2J_1(\mu a)}{T_0\mu^3 aJ_0(\mu a)}\right) - A_0 = 0 \quad (2.159)$$

Simplifying equation (2.173) by dividing through by $A_0$ and making $J_0(\mu a)$=1 and $\frac{J_1(\mu a)}{\mu a}$ = 0.5 because of the asymptote values are easier to approximate.

$$\psi_{11} = \left(-\frac{\rho\omega_c^2(\frac{H}{R}+B_0)}{T_0\mu^2}\right) + \left(\frac{\rho\omega_c^2(\frac{H}{R}+B_0)2J_1(\mu a)}{T_0\mu^3 aJ_0(\mu a)}\right) - 1 \quad (2.160)$$

Similarly, from equation (2.156) yields equation (4.1)

$$-i\omega_c\left(\frac{\rho i\omega_c A_n(e^{-k_n\frac{H}{R}} + B_n e^{k_n\frac{H}{R}})}{T_0\mu^2}\right)\left(\frac{J_0(k_n a)}{J_0(\mu a)}\right)\left(\frac{2J_1(\mu a}{a\mu}\right) = 0 \quad (2.161)$$

The coefficient of $\psi_{12}$ yields to equation (4.2) when $n$=1

$$\psi_{12} = \left(\frac{2\rho\omega_c^2(e^{-k_n\frac{H}{R}} + B_1 e^{k_n\frac{H}{R}})J_0(k_1 a)J_1(\mu a)}{T_0 a\mu\mu^2 J_0(\mu a)}\right) \quad (2.162)$$

When equation (4.1) has $n$=2

$$\psi_{13} = \left(\frac{2\rho\omega_c^2(e^{-k_n\frac{H}{R}} + B_2 e^{k_n\frac{H}{R}})J_0(k_2 a)J_1(\mu a)}{T_0 a\mu\mu^2 J_0(\mu a)}\right) \quad (2.163)$$

From equation (2.156) comparing coefficients yields equation (4.4)

$$i\omega_c\left(\frac{\rho i\omega_c A_0(\frac{H}{R}+B_0)}{T_0\mu^2}\right)\left(\frac{-2\mu J_1(\mu a)}{a(J_0\mu a)}\right)\sum_{m=1}^{\infty}\left(\frac{1}{(\mu^2-k_m^2)}\frac{J_0(k_m\frac{r}{R})}{J_0(k_m a)}\right) = 0 \quad (2.164)$$

when n = 1 and n =2 yields

$$\psi_{21} = \frac{2\rho\omega_c^2(\frac{H}{R} + B_0)J_1(\mu a)}{T_0\mu a J_0(\mu a)(\mu^2 - k_1^2)J_0(k_1 a)} \tag{2.165}$$

$$\psi_{31} = \frac{2\rho\omega_c^2(\frac{H}{R} + B_0)J_1(\mu a)}{T_0\mu a J_0(\mu a)(\mu^2 - k_2^2)J_0(k_2 a)} \tag{2.166}$$

Following the same procedure of comparing the coefficients of $A_0$ and $A_n$

$$\psi_{22} = \frac{2\rho\mu\omega_c^2(e^{-k_1\frac{H}{R}} + B_1 e^{k_1\frac{H}{R}})J_1(\mu a)}{T_0\mu a(\mu^2 - k_1^2)} - \frac{\rho\omega_c^2(e^{-k_n\frac{H}{R}} + B_1 e^{k_1\frac{H}{R}})}{T_0(\mu^2)} - \frac{k_1}{R}(e^{-k_1\frac{H}{R}} + B_1 e^{k_1\frac{H}{R}}) \tag{2.167}$$

$$\psi_{33} = \frac{2\rho\mu\omega_c^2(e^{-k_2\frac{H}{R}} + B_2 e^{k_2\frac{H}{R}})J_1(\mu a)}{T_0\mu a(\mu^2 - k_2^2)} - \frac{\rho\omega_c^2(e^{-k_2\frac{H}{R}} + B_2 e^{k_2\frac{H}{R}})}{T_0(\mu^2)} - \frac{k_2}{R}(e^{-k_2\frac{H}{R}} + B_2 e^{k_2\frac{H}{R}}) \tag{2.168}$$

Finally,

$$\psi_{23} = \frac{2\mu\rho\omega_c^2(e^{-k_2\frac{H}{R}} + B_2 e^{k_2\frac{H}{R}})J_0(k_2\frac{r}{R})J_1(\mu a)}{T_0 a(\mu^2)(\mu^2 - k_1^2)J_0(k_1 a)J_0(\mu a)} \tag{2.169}$$

$$\psi_{32} = \frac{2\mu\rho\omega_c^2(e^{-k_1\frac{H}{R}} + B_1 e^{k_1\frac{H}{R}})J_0(k_1\frac{r}{R})J_1(\mu a)}{T_0(\mu^2)J_0(k_2 a)(\mu^2 - k_2^2)J_0(\mu a)} \tag{2.170}$$

The determinant of the $C$ matrix below gives the required coupled frequency or frequency determinant obtained by solving the set of simultaneous equation 2.156.

$$C = \begin{vmatrix} \psi_{11} & \psi_{12} & \psi_{13} & \dots \\ \psi_{21} & \psi_{22} & \psi_{23} & \dots \\ \psi_{31} & \psi_{32} & \psi_{33} & \dots \\ \vdots & \vdots & \vdots & \vdots \end{vmatrix}$$

## 2.6. ANALYSIS OF COUPLED FLUID-STRUCTURE INTERACTION (MEMBRANE SUBMERGED)

In this section, linear theory is considered for better understanding of the fluid-structure interaction phenomenon.Moreover, in order to fully grasp what fluid-structure interaction is in its basic form, experimental processes such as viscosity, liquid surface tension are ignored.

The final coupled equation submerged membrane is determined by combining the coupled equations for when the membrane is at the top and at the bottom, for the final formulation for a submerged membrane. See figure 2.8.

From the compatibility equations from equations (2.136) and (2.72) , rewriting this yields

$$\frac{\partial w}{\partial t} - \frac{\partial \phi}{\partial z}\Big|_{z=0} = \frac{\partial w}{\partial t} - \frac{\partial \phi}{\partial z}\Big|_{z=H} \tag{2.171}$$

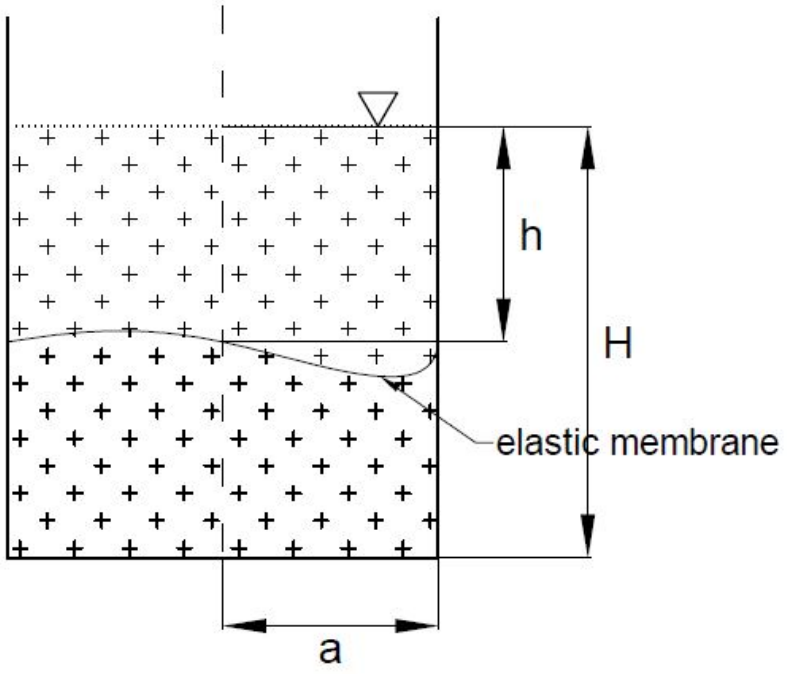


Figure 2.8: Description of the coupling phenomenon with membrane located at the top of the cylinder 3-D case

$$
\begin{aligned}
i\omega\gamma_0\prime - i\omega\gamma_0\prime\frac{2J_1(\mu a)}{a\mu J_0(\mu a)} - i\omega\gamma_0\prime\frac{2\mu J_1(\mu a)}{aJ_0(\mu a)}\sum_{m=1}^{\infty}\frac{1}{(\mu^2-k_m^2)}\frac{J_0(k_m r)}{J_0(k_m a)} + \sum_{n=1}^{\infty} i\omega\gamma_n\prime J_0(k_n r) \\
- \sum_{n=1}^{\infty} i\omega\gamma_n\prime\frac{J_0(k_n a)}{J_0(\mu a)}\frac{2J_1(\mu a)}{a\mu} - \sum_{n=1}^{\infty} i\omega\gamma_n\prime\frac{J_0(k_n a)}{J_0(\mu a)}\sum_{m=1}^{\infty}\frac{2\mu J_1(\mu a)J_0(k_m r)}{a(\mu^2-k_m^2)J_0(k_m a} \\
- A_0 - \sum_{n=1}^{\infty} k_n A_n\,(B_n - 1)\,J_0(k_n r) \\
= \quad i\omega\delta_0\prime - i\omega\delta_0\prime\frac{2J_1(\mu a)}{a\mu J_0(\mu a)} - i\omega\delta_0\prime\frac{2\mu J_1(\mu a)}{aJ_0(\mu a)}\sum_{m=1}^{\infty}\frac{1}{(\mu^2-k_m^2)}\frac{J_0(k_m r)}{J_0(k_m a)} + \sum_{n=1}^{\infty} i\omega\delta_n\prime J_0(k_n r) \\
- \sum_{n=1}^{\infty} i\omega\delta_n\prime\frac{J_0(k_n a)}{J_0(\mu a)}\frac{2J_1(\mu a)}{a\mu} - \sum_{n=1}^{\infty} i\omega\delta_n\prime\frac{J_0(k_n a)}{J_0(\mu a)}\sum_{m=1}^{\infty}\frac{2\mu J_1(\mu a)J_0(k_m r)}{a(\mu^2-k_m^2)J_0(k_m a} \\
- A_0 - \sum_{n=1}^{\infty} k_n A_n\left(B_n e^{k_n H} - e^{-k_n H}\right)J_0(k_n r) \qquad (2.172)
\end{aligned}
$$

From the above equation (2.172) by comparing coefficients, the elements of the matrix are below

$$
i\omega\gamma_0\prime - i\omega\gamma_0\prime\frac{2J_1(\mu a)}{a\mu J_0(\mu a)} - A_0 = i\omega\delta_0\prime - i\omega\delta_0\prime\frac{2J_1(\mu a)}{a\mu J_0(\mu a)} - A_0 \qquad (2.173)
$$

Similarly, following the equation 2.172, the elements of the matrix are as follows.

$$\xi_{11} = \frac{\rho\omega^2 B_0}{T_0\mu^2} - \frac{\rho\omega^2 B_0}{T_0\mu^2}\frac{2J_1(\mu a)}{a\mu J_0(\mu a)} + \frac{\rho\omega^2(H+B_0^t)}{T_0\mu^2} - \frac{\rho\omega^2(H+B_0^t)2J_1(\mu a)}{T_0\mu^2 a\mu J_0(\mu a)}$$

$$\xi_{12} = \frac{-2\rho\omega^2(1+B_1)J_0(k_1a)J_1(\mu a)}{T_0 a\mu(\mu^2-k_1^2)J_0(\mu a)} - \frac{2\rho\omega^2(e^{-k_1H}+B_1^t e^{k_1H})J_0(k_1a)J_1(\mu a)}{T_0 a\mu(\mu^2-k_1^2)J_0(\mu a)}$$

$$\xi_{13} = \frac{-2\rho\omega^2(1+B_2)J_0(k_2a)J_1(\mu a)}{T_0 a\mu(\mu^2-k_2^2)J_0(\mu a)} - \frac{2\rho\omega^2(e^{-k_2H}+B_2^t e^{k_2H})J_0(k_2a)J_1(\mu a)}{T_0 a\mu(\mu^2-k_2^2)J_0(\mu a)}$$

$$\xi_{21} = \frac{-2\rho\omega^2 B_0 J_1(\mu a)}{T_0\mu a(\mu^2-k_1^2)J_0(k_1a)J_0(\mu a)} - \frac{2\rho\omega^2(H+B_0^t)J_1(\mu a)}{T_0\mu a(\mu^2-k_1^2)J_0(k_1a)J_0(\mu a)}$$

$$\xi_{22} = \frac{-2\rho\mu\omega^2(1+B_1)J_1(\mu a)}{T_0 a\left(\mu^2-k_1^2\right)^2 J_0(\mu a)} + \frac{\rho\omega^2(1+B_1)}{T_0\left(\mu^2-k_1^2\right)} - k_1(B_1-1) - \frac{2\rho\mu\omega^2(e^{-k_1H}+B_1^t e^{k_1H})J_1(\mu a)}{T_0 a\left(\mu^2-k_1^2\right)^2 J_0(\mu a)} + \frac{\rho\omega^2(e^{-k_1H}+B_1^t e^{k_1H})}{T_0\left(\mu^2-k_1^2\right)} + k_1\left(e^{-k_1H}-B_1^t e^{k_1H}\right)$$

$$\xi_{23} = \frac{-2\rho\mu\omega^2(1+B_2)J_0(k_2a)J_1(\mu a)}{T_0 a(\mu^2-k_1^2)J_0(k_1a)(\mu^2-k_2^2)J_0(\mu a)} - \frac{2\rho\mu\omega^2(e^{k_2H}+B_2^t e^{k_2H})J_0(k_2a)J_1(\mu a)}{T_0 a(\mu^2-k_1^2)J_0(k_1a)(\mu^2-k_2^2)J_0(\mu a)}$$

$$\xi_{31} = \frac{-2\rho\omega^2 B_0 J_1(\mu a)}{T_0\mu a(\mu^2-k_2^2)J_0(k_2a)J_0(\mu a)} - \frac{2\rho\omega^2(H+B_0^t)J_1(\mu a)}{T_0\mu a(\mu^2-k_2^2)J_0(k_2a)J_0(\mu a)}$$

$$\xi_{32} = \frac{-2\rho\mu\omega^2(1+B_1)J_0(k_1a)J_1(\mu a)}{T_0 a(\mu^2-k_2^2)J_0(k_2a)(\mu^2-k_1^2)J_0(\mu a)} - \frac{2\rho\mu\omega^2(e^{k_1H}+B_1^t e^{k_1H})J_0(k_1a)J_1(\mu a)}{T_0 a(\mu^2-k_1^2)J_0(k_2a)(\mu^2-k_2^2)J_0(\mu a)}$$

$$\xi_{33} = \frac{-2\rho\mu\omega^2(1+B_2)J_1(\mu a)}{T_0 a\left(\mu^2-k_2^2\right)^2 J_0(\mu a)} + \frac{\rho\omega^2(1+B_2)}{T_0\left(\mu^2-k_2^2\right)} - k_2(B_2-1) - \frac{2\rho\mu\omega^2(e^{-k_2H}+B_2^t e^{k_2H})J_1(\mu a)}{T_0 a\left(\mu^2-k_2^2\right)^2 J_0(\mu a)} + \frac{\rho\omega^2(e^{-k_2H}+B_2^t e^{k_2H})}{T_0\left(\mu^2-k_2^2\right)} + k_2\left(e^{-k_2H}-B_2^t e^{k_2H}\right) \quad (2.174)$$

The terms with a superscript of **t** means the membrane is at the top. Similarly, the determinant of the matrix whose elements are highlighted above gives the required coupled frequency or frequency determinant obtained by solving the set of simultaneous equation (2.172).

$$\Xi = \begin{vmatrix} \xi_{11} & \xi_{12} & \xi_{13} & \cdots \\ \xi_{21} & \xi_{22} & \xi_{23} & \cdots \\ \xi_{31} & \xi_{32} & \xi_{33} & \cdots \\ \vdots & \vdots & \vdots & \vdots \end{vmatrix}$$

# 3

# RESULTS AND DISCUSSION

## 3.1. INTRODUCTION

The analysis of the model are discussed extensively in this chapter to explain the physical representation of this problem. This is of engineering interest to ease understanding. Building the model in steps, the dynamic behaviour of the freely vibrating string and membrane *In vacuo* are presented as well as the dynamics of the coupled Fluid-Structure Interaction (FSI) problem in 2-D and 3-D case. The understanding of this coupling phenomenon are judged mainly by visual inspection and testing of variables to see how they compares to the dry case and free surface frequencies when it is uncoupled.

## 3.2. DYNAMIC BEHAVIOUR OF FREELY VIBRATING STRING *In vacuo*

The frequency represented as $\omega = \frac{f\pi c}{l}$ depends upon the length, tension and mass of the string. The figure 3.1 below shows the vibration modes of a fixed-fixed string. The index $f$ = 1,2,3... shows that it is a continuous system having infinite number of natural frequencies[1]. The vibration mode are simply displacement patterns the string will possess at a distinct frequency, in this case it is sinusoidal in nature.

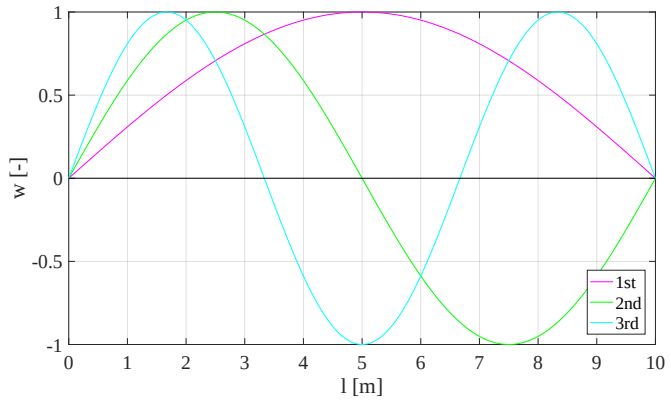


Figure 3.1: The first three vibration modes of a fixed-fixed string *In vacuo*

[1]The natural frequencies of a system is simply the frequency at which the system oscillates without any external excitation

## 3.3. DYNAMIC BEHAVIOUR OF FREELY VIBRATING CIRCULAR MEMBRANE *In vacuo*

The frequencies of a circular fixed membrane *In vacuo* from equation (2.27) is shown in the figure 3.2 below. The figure 3.2 below shows both the axisymmetric and asymmetric natural frequencies of the *In Vacuo* membrane. Since it is a continuous system, the natural frequency equation has infinitely many roots.

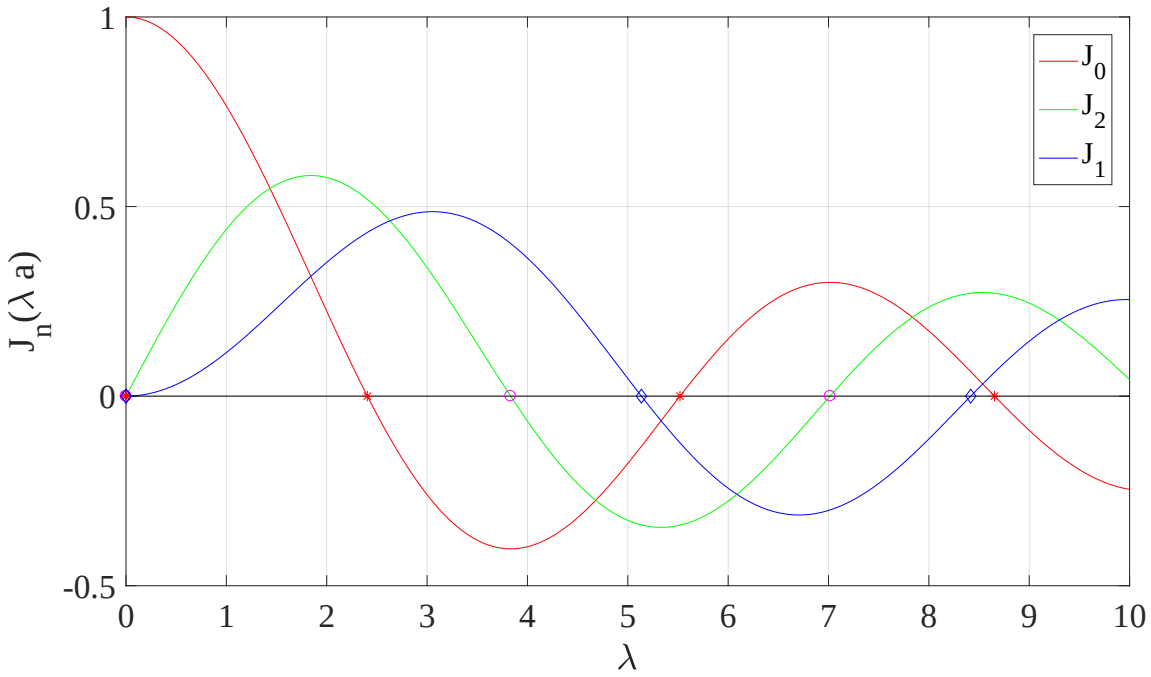


Figure 3.2: Plot showing the natural frequencies of a fixed circular membrane *In vacuo*.

Figure 3.2 above shows the natural frequencies of the membrane under fixed boundary condition from equation (2.27). The value of $n = 1,2,...$ means the nodes will be at the edges of the fixed membrane and it is the order of the Bessel function which dictates the frequency of the membrane. The difference between $J_0$ , $J_1$ and $J_2$ is simply the order of the Bessel function, however, the roots (zero-crossings) of the equation (2.27) in figure 3.2 gives the exact root or rank of the frequency. Table 3.1 gives a summary.

Table 3.1 below presents the non-dimensional frequencies $\lambda = (\frac{m}{T_o})^{\frac{1}{2}}\omega$ from equation (2.27) of the fixed edges first nine frequencies[2] With $m = 1,2,3$ and $n = 0,1,2$.

Thus, $\omega_{m,n} = \omega_{1,0} = 2.4048$, $\omega_{1,1} = 3.8317$, $\omega_{1,2} = 5.1356$.

This means at order 0 of the Bessel function (axisymmetric), the first frequency is 2.4048, the second frequency is 5.5201 and the third frequency is 8.6573.

[2]The natural frequency is dependent on the mass of membrane, radius of membrane and tension, the values of the frequency below in the table assumes a tension radius and mass of unity.

Table 3.1: The non-dimensional frequencies $\lambda = (\frac{m}{T_o})^{\frac{1}{2}}\omega$ of a circular fixed membrane *In vacuo*

| | $J_0$ | $J_1$ | $J_2$ |
|---|---|---|---|
| $m = 1$ | 2.4048 | 3.8317 | 5.1356 |
| $m = 2$ | 5.5201 | 7.0155 | 8.4172 |
| $m = 3$ | 8.6537 | 10.1735 | 11.620 |

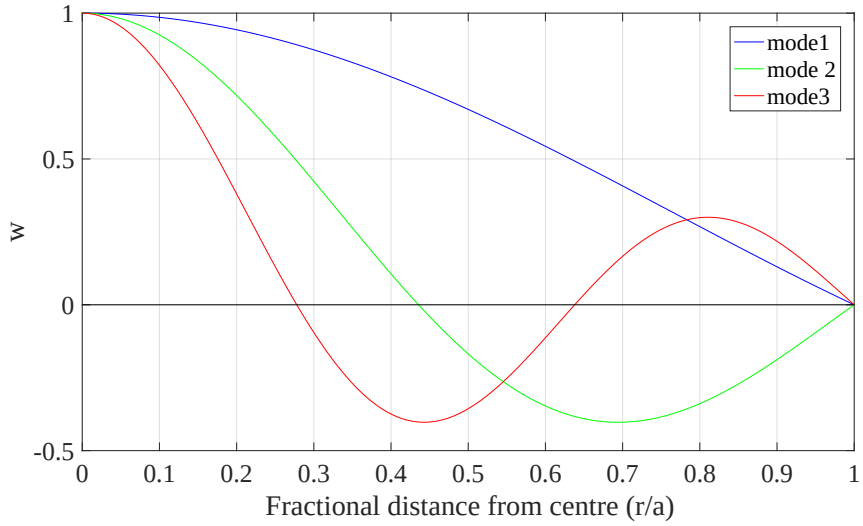


(a) vibration modes at $n = 0$, $m = 1, 2, 3$

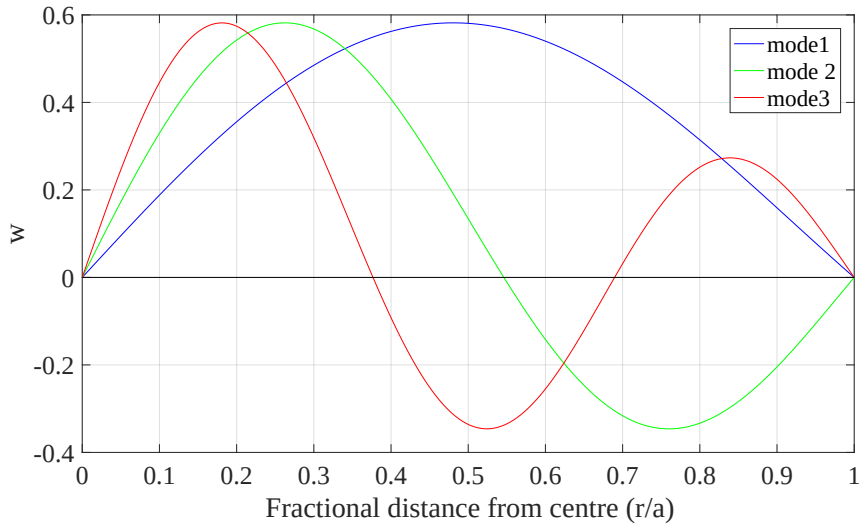


(b) vibration modes at $n = 1$, $m = 1, 2, 3$

Figure 3.3: Vibration modes of the freely vibrating circular membrane at $n$= 0, 1 and $m = 1, 2, 3$ respectively

From table 3.2 and 3.3 the values of the last column shows the radius of the nodal circles formed from the roots of the vibration modes as seen in figure 3.3 above. It is interesting to note that the nodal circles appears at a distinct frequency. Thus, when $n = 0$ and $m = 2$, i.e. zero nodal diameter and two nodal circles. The corresponding frequency which is 5.5202 and two nodal circles will be formed as the membrane vibrates at radius of 0.4357 and the second radius comes from the radius of the membrane. This corroborates the equation (2.11). More visualization is seen in figure B.1 in the appendix B

Table 3.2: First three non-dimensional frequencies and nodal circles $m = 1\ 2, 3,\ n = 0$ *In vacuo*

| s/n | Frequency | Nodal circle |
|---|---|---|
| 1 | 2.4048 | |
| 2 | 5.5202 | 0.4357 |
| 3 | 8.6537 | 0.2757 and 0.6375 |

Table 3.3: First three non-dimensional frequencies and nodal circles $m = 1\ 2, 3,\ n = 1$ *In vacuo*

| s/n | Frequency | Nodal circle |
|---|---|---|
| 1 | 3.8317 | |
| 2 | 7.0155 | 0.5462 |
| 3 | 10.1735 | 0.3766 and 0.6896 |

Figure 3.4 below shows a better appreciation of visualisation in 3-D of the membrane of the first two frequencies $m = 1, 2$ and $n = 1$.

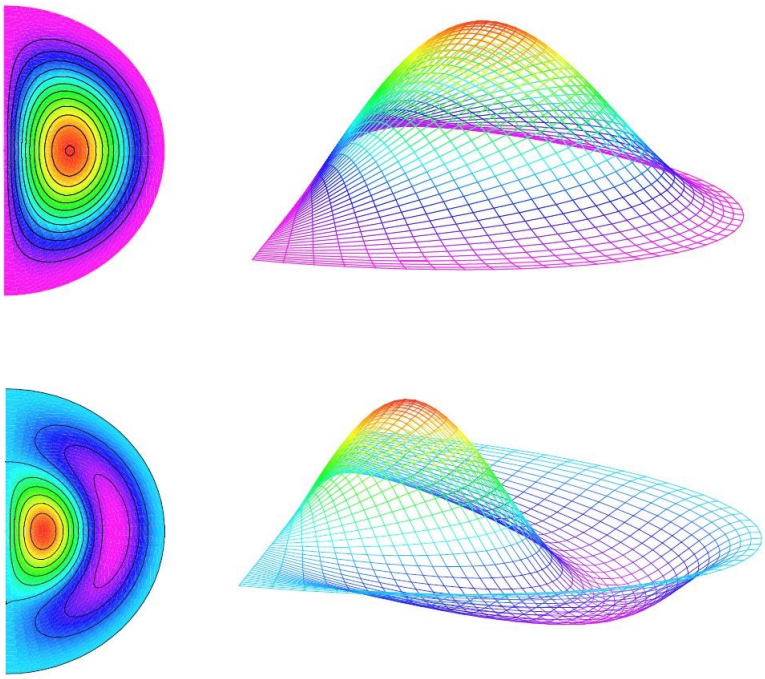

Figure 3.4: Vibration modes of first two frequencies with one nodal diameter *In vacuo* [4]

## 3.4. DYNAMIC BEHAVIOUR OF COUPLED FREQUENCY IN 2-D CASE

In understanding the behaviour of FSI, the characteristic equation in equation (2.63) is shown in the figure 3.5 below. Dealing with a continuous system, the coupled frequency has infinitely many frequencies. The roots of the frequency equations marked in * represents the coupled frequencies. The numerical values used are: $T = 500$ N/m, $m_s = 1$ kg/m.

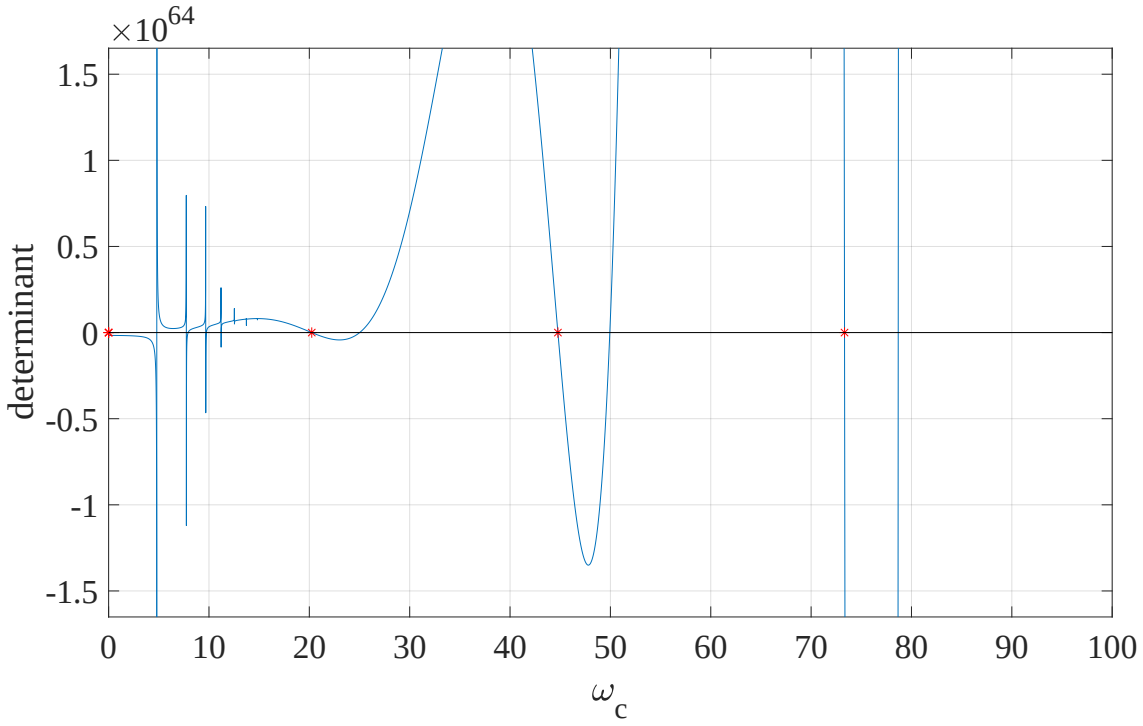


Figure 3.5: Plot of series equation as a function coupled frequencies in the 2-D case with $\frac{h}{b} = 0.3$

Figure 3.5 above, the plot of the characteristics equations behaves in an erratic manner: The coupled frequencies are of course as a result of the fluid-structure interaction, however, in investigating the vibration modes and comparing with the *In vacuo* case, the marked * , coupled frequencies follows the desired vibration modes which are sinusoidal as in the *In vacuo* caes. The other coupled frequencies observed are simply as a result of asymptotes that occur due to the coupling phenomenon. This doesn't mean the unmarked roots (zero-crossings) are not correct. It is believed that the fluid causes oscillations to occur on the membrane at lower observed frequencies. It is believed also that these low frequencies are predominantly the frequencies of the free surface and these lower frequency regions are roots of the denominator of equation (2.63). In table 3.4 below, the coupled frequencies of equation (2.63) are shown.

Table 3.4: First three coupled frequencies of a string and fluid free surface with $\frac{h}{b} = 0.3$ in 2-D case.

| s/n | 1 | 2 | 3 |
|---|---|---|---|
| Frequency (rad/s) | 20.241 | 44.769 | 73.329 |

From figure 3.5 above, the coupled frequencies are shown, the marked * couple frequencies which produce a sinusoidal vibration mode are 20.241 rad/s, 44.769 rad/s and 73.329 rad/s. These marked coupled frequencies exhibits the third, fifth and seventh mode respectively.

In an attempt to directly compare the coupled frequencies and the natural frequencies of the *In vacuo* case, it was observed that the coupled frequencies are lower at the lower regions see table 3.5. This is logical because of the added mass created by the fluid. However, at higher regions, the coupled frequency than to be larger than the *In Vacuo* frequency. This is simply due to stronger coupling effect from the fluid.

Table 3.5: Comparism of coupled and *In vacuo* frequencies in 2-D case.

| s/n | 1 | 2 | 3 |
|---|---|---|---|
| coupled frequency (rad/s) | 20.241 | 44.769 | 73.329 |
| *In Vacuo* frequency (rad/s) | 21.074 | 35.124 | 49.173 |

The vibration of the string and free surface using the coupled frequency is shown below in figure 3.6. Figure 3.6 below represents the vibration mode of the string and it shows the behaviour of the fluid free surface at the same frequency of $\omega_c$ = 20.241 rad/s. The fluid free surface exhibits a different vibration mode, this is mainly due to the time variable. Independent of time, the vibration modes of string and fluid free surface possess the same vibration mode shape. The reason for this behaviour can be explained mathematically, on solving the partial differential equations of the string coupled with the fluid, using the methods of variable separation. All variables, x, z and t are dealt with independently. It is established that fluid takes the shape(volume) of its container when all exciting forces are absent. When these variables are considered together, the vibration mode of the free surface is different as seen in figure 3.6.

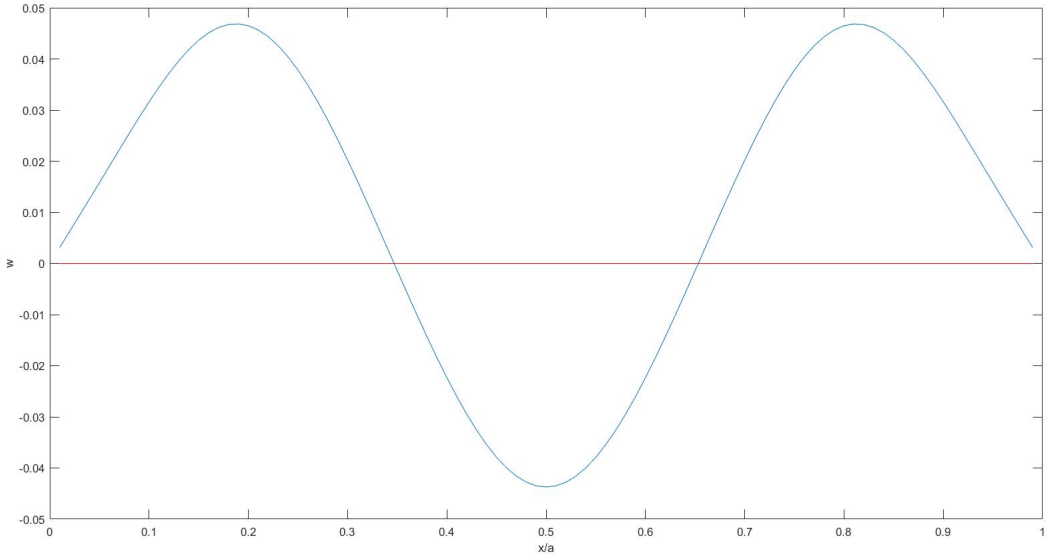


(a) string modes

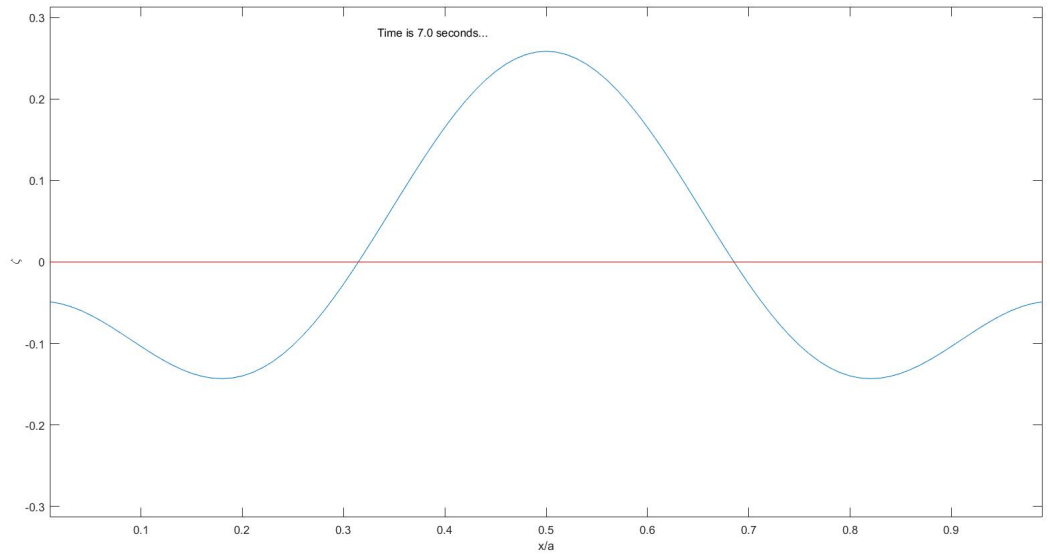


(b) fluid free surface modes

Figure 3.6: Vibration modes of the string and fluid free surface at 7th frequency with $\omega_c$ = 20.241rad/s

## 3.5. DYNAMIC BEHAVIOUR OF COUPLED FREQUENCY IN 3-D CASE

In understanding the behaviour of FSI in 3-D, two cases are considered: The first case considers the situation where the membrane is located at the bottom of the cylinder and the second case considers a membrane located at the top of the bigger cylinder and completely ignoring the smaller cylinder.

### 3.5.1. MEMBRANE LOCATED AT THE BOTTOM OF THE SMALLER CYLINDER

The coupled frequency is a function of the determinant of $A$ matrix from equation (2.91). The $A$ matrix captures only axisymmetric vibration modes. The parameters used are: $h/a = 0.3$, $T_o = 500$ N/m, $m_m = 1$ kg/m, $a = 1$ m. The coupled frequencies are the roots of the solution to the determinant of the $A$ matrix. It is expected that the coupled frequency consist of infinitely many values since it is a continuous system, thus truncating the infinite determinant is advantageous, subsequently producing a finite number of rows and columns that yields an approximate set of solutions of coupled frequencies.

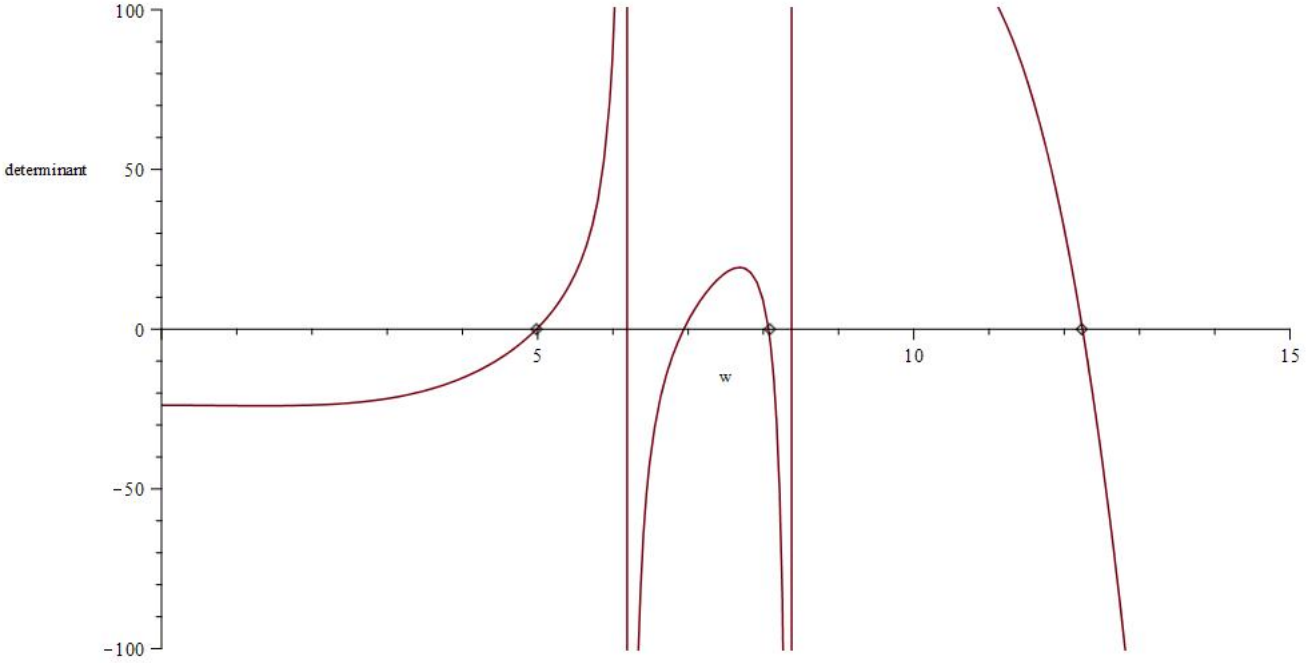


Figure 3.7: Plot of determinant as a function of coupled frequency. The zero-crossing represents solution to $|A| = 0$

Figure 3.7 above, the abscissa axis is the coupled frequency ($\omega_c$) and the ordinate axis is the determinant of ($A$ matrix). The roots of the equation gives the coupled frequency up to the first four frequencies as shown in table 3.6. From the figure 3.7, the roots marked in ◇ shows the desired coupled frequencies. From table 3.6, it should be noted that not all coupled frequency gives the desired vibration mode, it is simply due to the nonlinear behaviour of the fluid and membrane, this is judged by plotting the vibration modes and comparing with the *In vacuo* case.

Table 3.6: First four non-dimensional coupled frequencies $\mu^2 = \frac{m_m}{T_o}\omega_c^2$ of membrane located at the bottom of the cylinder

| s/n | 1 | 2 | 3 |
|---|---|---|---|
| Frequency | 4.984 | 8.086 | 12.232 |

The amplitude of membrane and free surface are dependent on $A_0$ and $A_n$ from equation(2.91). For better understanding of these concept, the amplitudes were ignored because they are constants and are of little engineering importance, as it only reduces the scale of the plots. It is highly recommended that all values of the roots (coupled frequencies $\omega_c$) be checked. For example, the value of second frequency from figure 3.7 given as 6.967, though a root of equation (2.91) does not give a reliable vibration mode of the membrane when compared to the *In vacuo* case. It was observed that the vibration mode attached to that frequency was simply a build up of the desired vibration mode obtained in 8.086. Hence, it is believed that the behaviour of the coupled frequencies and vibration modes are influenced by the fluid-structure interaction coupling. This simply means that coupled frequencies close to each other will likely exhibit similar vibration patterns. See reference to **implicit plot**[3] in appendix A.

Extending the abscissa axis, the next coupled frequency observed was 128.243 which is the $41^{st}$ vibration mode, high frequency regions. This is the main reason for truncating the set of solutions for easier understanding and monitoring of the coupled frequency.

It is note worthy also, that in the coupled case, by comparing the vibration modes of *In vacuo* case, the first vibration mode of the *In vacuo* case is absent from the coupled case. it is believed that this vibration mode is a bulging mode of the membrane and not a sloshing mode caused solely by the free surface. Figure 3.8 shows the vibration modes of the membrane and fluid free surface at coupling frequencies from table 3.6.

Table 3.7: Comparison of coupled, *In vacuo* and fluid free surface frequencies parameters with $h/a = 0.3, T_o = 500\text{N/m}$, $m_m = 1\text{kg/m}$, $a = 1\text{m}$ of a circular membrane located at the bottom

| s/n | 1 | 2 | 3 |
|---|---|---|---|
| Coupled frequency($\omega_c$ ) | 4.984 | 8.086 | 12.232 |
| *In Vacuo* frequency ($\omega$) | 5.5202 | 8.6537 | 11.790 |
| Fluid free surface frequency ($\omega_s$) | 5.543 | 8.1736 | 9.967 |

From table 3.7 above, the coupled frequency represented by $\omega_c$ give lower frequencies than *In vacuo* frequencies represented by $\omega$ and even lower frequencies compared to the fluid free surface frequency represented by $\omega_s$.

[3]Implicit plots are methods employed to verify the results of the coupled frequencies

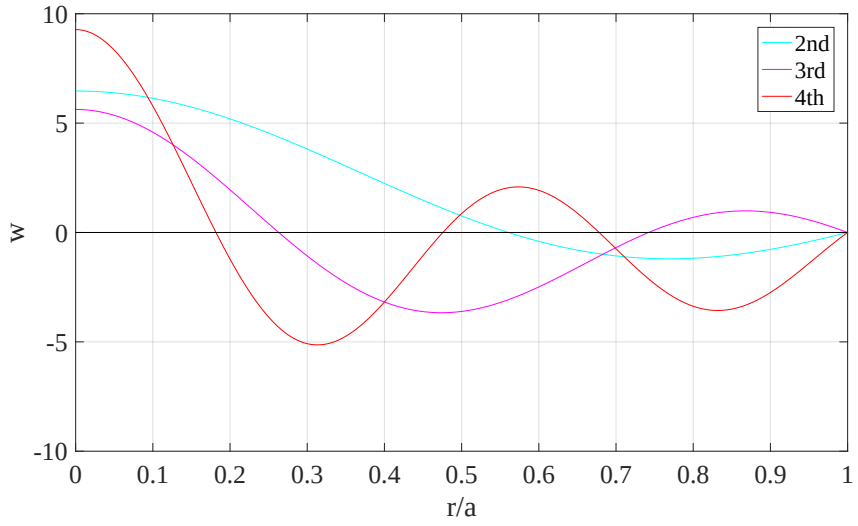


(a) Membrane modes

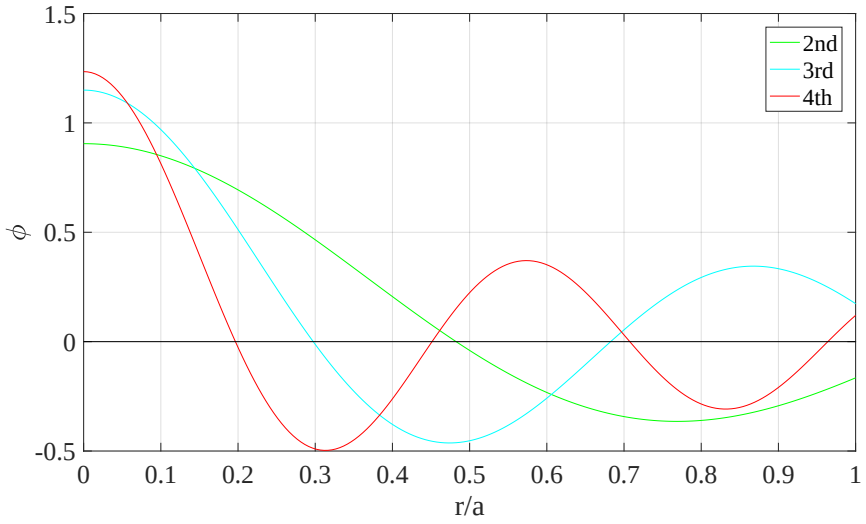


(b) Fluid free surface modes

Figure 3.8: Vibration modes of the membrane and fluid free surface at first three coupled frequencies for axisymmetric case $n$= 0, $m$ = 2,3,4 of membrane located at the bottom

### 3.5.2. MEMBRANE LOCATED AT THE TOP OF BIGGER CYLINDER

The coupled frequency is a function of the determinant matrix $C$. The $C$ matrix captures only axisymmetric mode shapes. The coupled frequencies are the roots to the determinant of the $C$ matrix. As observed, the coupled frequency increased due to a higher water depth. It may also be mentioned that a substantial mass of the membrane must be considered, (**using** $H/a$ = 2.0**,** $T_o$ = 500 **N/m,** $m_m$ = 1 **kg/m,** $a$ = 1 **m**) because the water depth is really high in magnitude, reducing this water depth, a considerable level of oscillation was observed as vibrations reaching the membrane. Hence, this is the most singular factor that affects the fluid-membrane interaction. In summary, increasing the water depth yields an increase in coupled frequencies. Nevertheless, with an increase in the water depth, wave particles tend to oscillate so much causing higher coupled frequencies. Increasing the tension of the membrane compensates for large water depth as it reduces the coupled frequency parameter $\mu^2 = \dfrac{m_m}{T_o}\,\omega_c^2$ from equation(2.150). For this study, a considerable mass and tension were used, thus, 2624.805 kg/m and 1785.82 N/m respectively. The computation used in this case, $a = R$, see figure 2.7 for easy understanding of the coupled frequencies when the membrane is suited at the top.

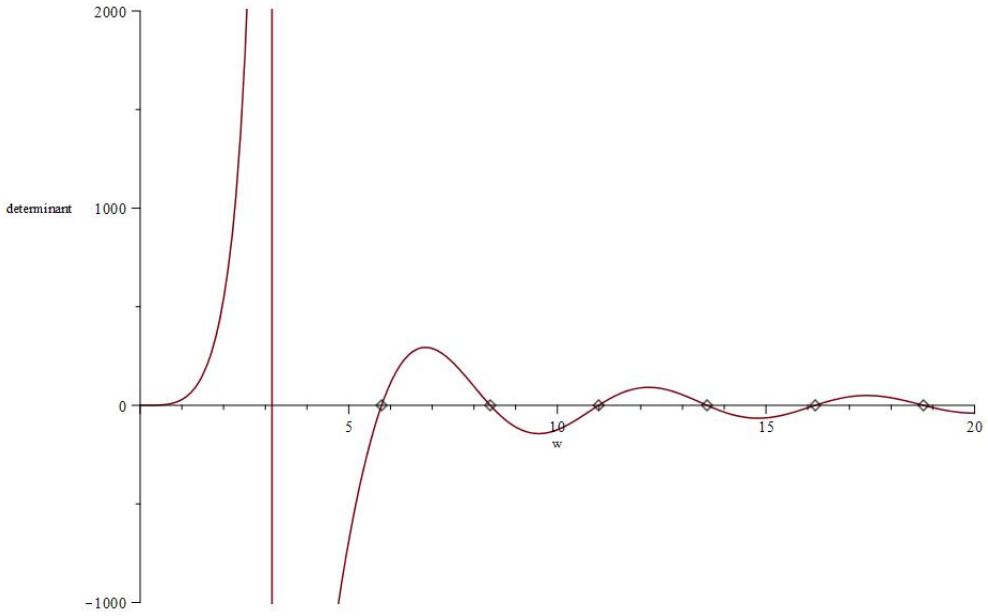


Figure 3.9: Plot of determinant as a function of coupled frequency. The zero-crossing represents solution to $|C| = 0$

By visual inspection of figures 3.9 and figure 3.7 above, it is seen that the non-dimensional coupled frequency are larger in magnitude when the membrane is located at the top than when membrane is located at the bottom marked by the $\diamond$ shape.

Table 3.8: First six non dimensional coupled frequencies $\mu^2 = \dfrac{m_m}{T_o}\,\omega_c^2$ with membrane located at the top

| s/n | 1 | 2 | 3 | 4 | 5 | 6 |
|---|---|---|---|---|---|---|
| Frequency | 5.786 | 8.392 | 10.99 | 13.586 | 16.18 | 18.774 |

Similarly, the undesired vibration modes was also observed, as not all the roots of the from table 3.8 above gives desired mode shape, the term "desired mode shape" refers to vibration modes that gives similar vibration patterns observed from when the membrane is dry that is *In vacuo*. This is the

major yardstick to judge the observed vibration modes observed from the coupling phenomenon of fluid-structure interaction. Figure 3.10 below shows the vibrations patterns of the first three modes.

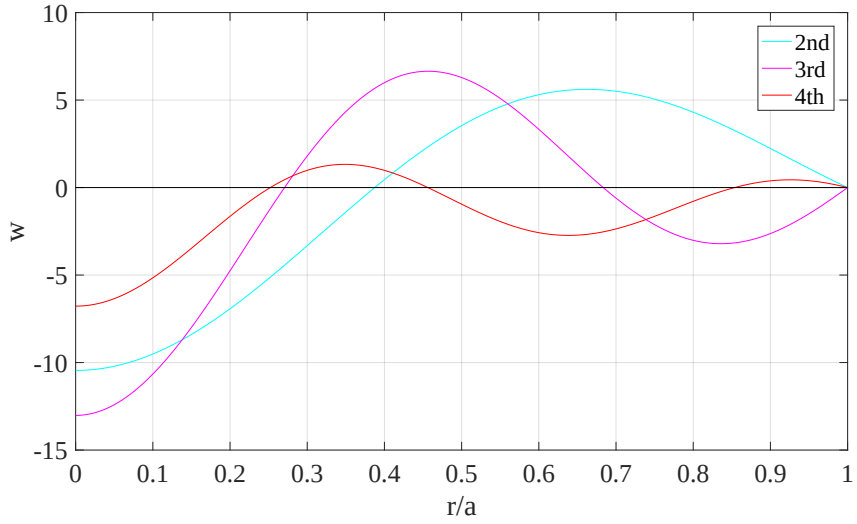


(a) Membrane modes

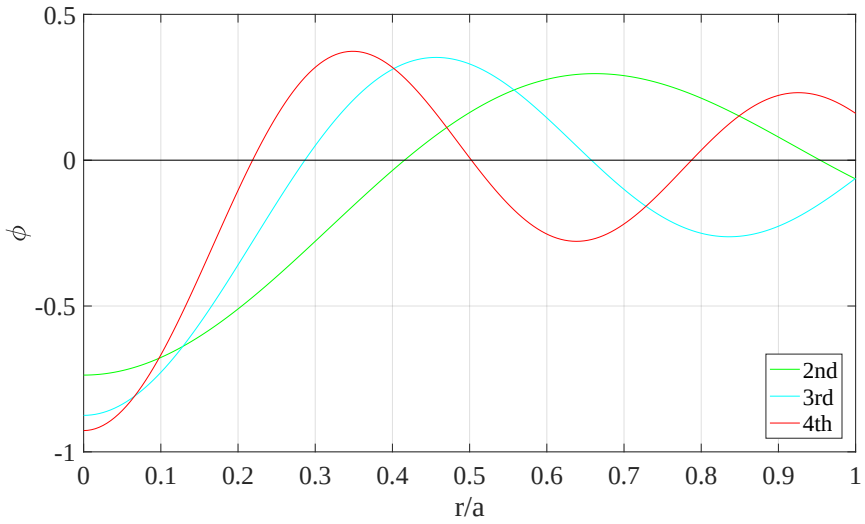


(b) Fluid free surface modes

Figure 3.10: Vibration modes of the membrane and fluid free surface at first three coupled frequencies for axisymmetric case $n = 0$, $m = 2,3,4$ for membrane located at the top

## 3.6. DYNAMIC BEHAVIOUR OF COUPLED FREQUENCY OF A SUBMERGED MEMBRANE 3-D CASE

The roots of the determinant matrix $\Xi$ gives the coupled frequencies of the submerged membrane. For this numerical result, the values of the parameters are: $H/a = 2.0$, $h/a = 0.3$, $T_o = 1785.82$N/m, $m_m = 2624.805$kg/m, $a = 2$m. Where $H$ is height of the water column of the bigger cylinder, $h$ is the height of the water column of the smaller cylinder and a is the radius of the membrane.

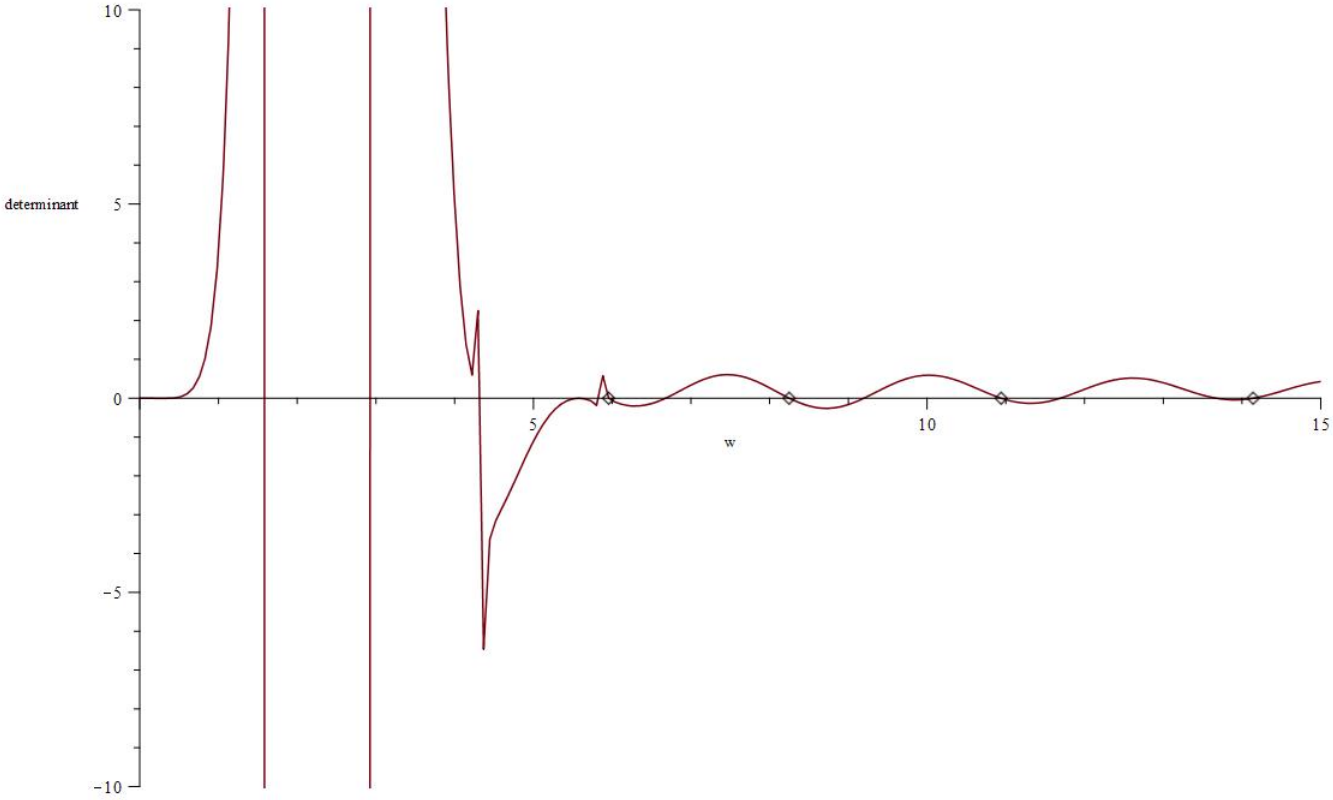


Figure 3.11: Plot of determinant as a function of coupled frequency. The zero-crossing represents solution to $|\Xi| = 0$

Figure 3.11 above,it depicts the plot of the coupled frequencies of a submerged membrane as a function of the determinants. The roots are marked by the $\diamond$ shape. The values of the coupled frequency are given in the table 3.9 below.

Table 3.9: First four non dimensional coupled frequencies $\mu^2 = \frac{m_m}{T_o}\omega_c^2$ of a submerged circular membrane

| s/n | 1 | 2 | 3 | 4 |
|---|---|---|---|---|
| Frequency | 5.956 | 8.248 | 10.94 | 14.14 |

It should be mentioned that the free surface vibration mode is the algebraic sum of the membrane situated at the top and bottom. This is because the free surface vibration mode is a function of the height of the water column. The fluid pressure loads acting on the membrane located at the top is opposite at the membrane located at the bottom of the cylinder. Figure 3.12 below shows the vibration patterns of the submerged membrane and fluid free surface at coupled frequencies.

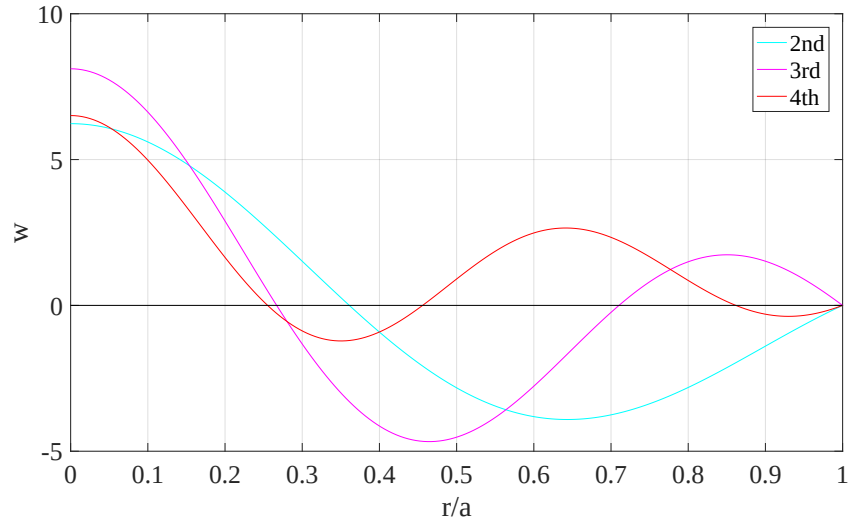


(a) Membrane modes

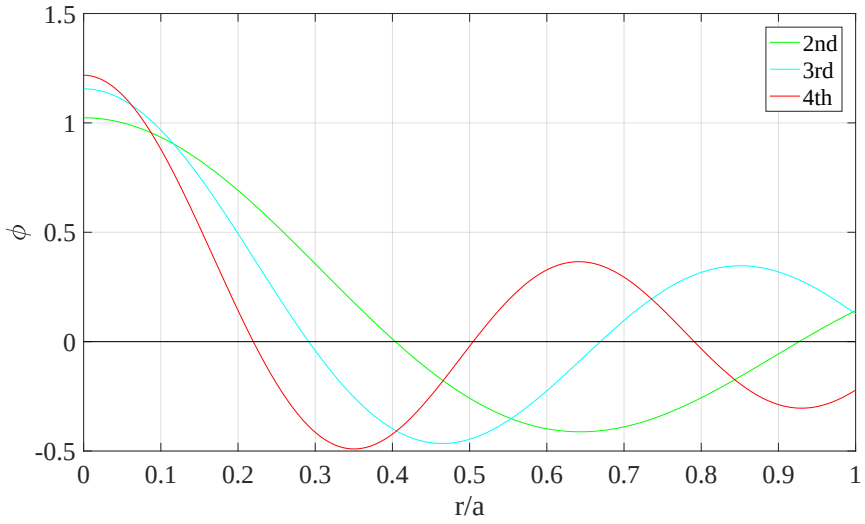


(b) Fluid free surface modes

Figure 3.12: Vibration modes of the membrane and fluid free surface at first three coupled frequencies for axisymmetric case $n = 0$, $m = 2,3,4$ for a submerged membrane

# 4

# VERIFICATION

## 4.1. INTRODUCTION

This sections deals mainly with testing the equation parameters to verify if the equations solved in chapter 2 were done rightly. This entails making modifications to the coupled equations to capture the *In vacuo* case

## 4.2. VERIFICATION OF EQUATIONS: MEMBRANE LOCATED AT THE BOTTOM OF CYLINDER

The verification and results in this chapter are only done using the axisymmetric case, that is the nodal diameter are not considered to affect the coupled frequency, thus, $n$=0 and $m = 1$. The reason for this is, to reduce the computational process and fully grasps the coupling phenomenon of fluid-structure interaction.

From Matrix $A$ the coupled natural frequency obtained from set of simultaneous equations in equation (2.91) and the determinant of these equations yields the coupled frequencies. To verify Matrix $A$, judging from equation (2.91), if the tension of the membrane tends to infinity and the density of the liquid tends to zero individually, the frequency determinant becomes

$$J_0(\mu a)\prod_{n=1}^{\infty} k_n(B_n - 1) = 0 \tag{4.1}$$

From equation (4.1), If $J_0(\mu a)$=0: it is the same as with equation (2.27) which is the frequency of a dry membrane. Also, if $k_n(B_n - 1) \neq 0$, however, when $B_n = 1$ judging from equation (2.42), a dispersion relationship is obtained

$$\omega^2 = g k_n \left( \frac{e^{k_n h} - e^{-k_n h}}{e^{-k_n h} + e^{k_n h}} \right) = g k_n \tanh(k_n h) \tag{4.2}$$

Equation (4.1); it shows the frequency of a membrane without water see equation (2.27) and from equation (4.2), it shows the frequency of a rigid tank i.e. tension tending towards infinity at an infinite depth of water that eventually yield to $\omega^2 = g k_n$: this is not obtainable in this case because equation (2.72) is not obeyed. This is because the dispersion relationship is only obeyed when the $\frac{\partial \phi}{\partial z} = 0$ at $z$=0. The so called seabed boundary condition.

Judging from uncoupling of the system, the membrane natural frequency is obtained from equation (2.27). However, with additional (non-sloshing) liquid mass on the membrane, the uncoupled natural frequencies will be

$$\omega = \lambda \sqrt{\left(\frac{T}{m_m + \frac{h}{a}}\right)} \tag{4.3}$$

Where $\lambda$ is the root of equation (2.27) indicating a decrease of the frequency due to the liquid mass, as the water depth to radius of membrane ratio $\frac{h}{a}$ increase[1]. The uncoupled fluid free surface frequency is the given as

$$\omega_s^2 = \frac{g}{a} k_n \tanh\left(k_n \frac{h}{a}\right) \tag{4.4}$$

$k_n$ is the root of the equation (2.77)

## 4.3. BEHAVIOUR OF TENSION WITH RESPECT TO COUPLED FREQUENCY

Following the axisymmetric case, a very interesting behaviour was observed in the figure 4.1 and table 4.1 below. Keeping water depth to radius of membrane ratio $\frac{h}{a}$ constant, an increase in the tension, causes an increase in the coupled frequency, as seen in table 4.1. The oscillations of wave particle reduces as the membrane becomes stiffer, the fluid particles are not felt at the bottom. Figure 4.1 shows that an increase in tension, the coupled frequency tends towards the uncoupled membrane and uncoupled fluid free surface frequency.

Table 4.1: First three non dimensional coupled frequencies $\mu^2 = \frac{m_m}{T_o}\omega_c^2$ with respect to an increase in tension

| $T_o$ | 250 | 500 | 750 | 1000 |
|---|---|---|---|---|
| $1^{st}$ frequency | 4.099 | 4.280 | 4.949 | 5.114 |
| $2^{st}$ frequency | 6.655 | 7.554 | 7.512 | 8.091 |
| $3^{st}$ frequency | 7.195 | 8.017 | 8.185 | 8.217 |

[1] The $\frac{h}{a}$ ratio, that is water depth in cylinder to radius of the membrane in axisymmetric case is the representation of water depth to wave length of the water particles respectively. This important ratio is what determines the wave particle behaviour (frequency) this is known as called Linear or Airy Wave Theory

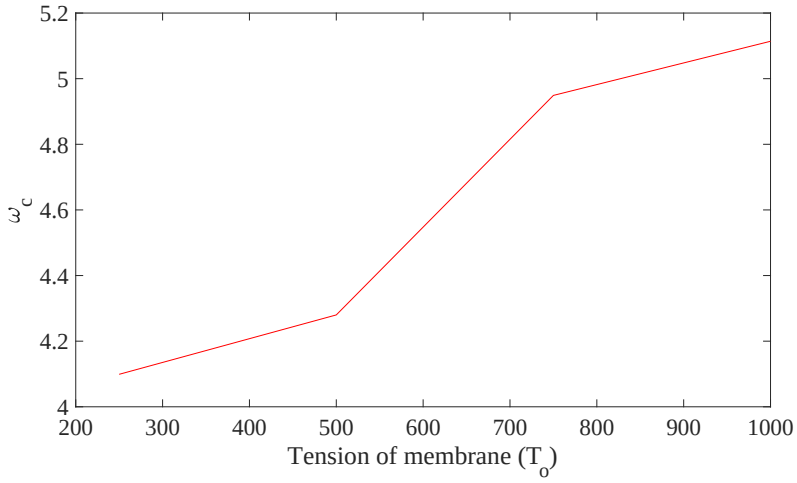


Figure 4.1: Relationship between coupled frequency and Tension

## 4.4. BEHAVIOUR OF THE WATER DEPTH TO RADIUS OF MEMBRANE RATIO $\frac{h}{a}$ WITH RESPECT TO COUPLED FREQUENCY 3-D

Considering the axisymmetric case, in figure 4.2 below, keeping the tension of the membrane constant and increasing the water depth $\frac{h}{a}$ causes a corresponding increase in the coupled frequency. The oscillation of the fluid increases because at low $\frac{h}{a}$ ratios, there is less fluid-structure interaction and at a higher $\frac{h}{a}$ ratio, there is more fluid-structure interaction.

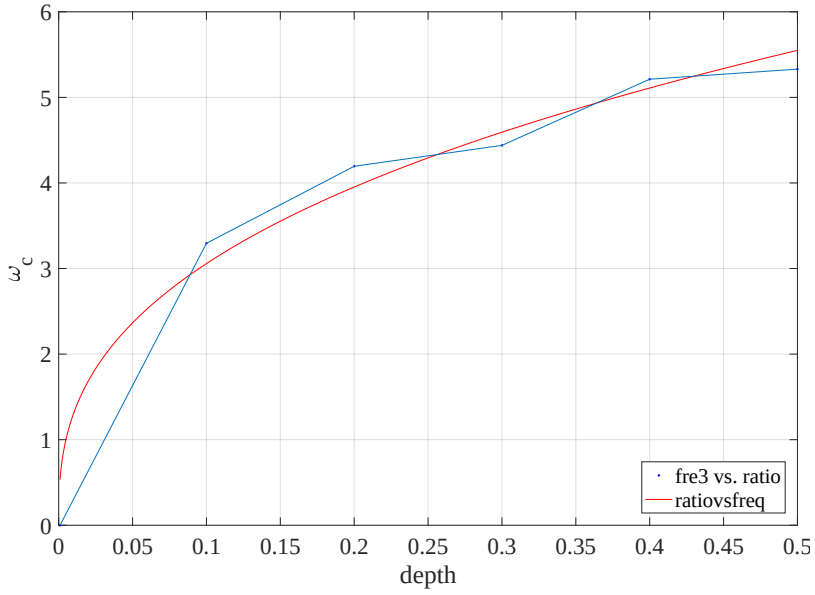


Figure 4.2: Relationship between coupled frequency and non-dimensional fluid depth
$m$=1 and $n$=0 axisymmetric case

Figure 4.2 above, the fluid depth to radius of the membrane ratio is on the abscissa and coupled frequency is on the ordinate axis. It shows that there is a convergence to the fluid free surface fre-

quency as seen from table 3.7. The fluid-structure interaction introduces an inconsistent behaviour also. With respect to uncoupled frequency of membrane and fluid, judging from equations (4.3) and (4.4) as the $\frac{h}{a}$ ratio increases the uncoupled membrane frequency reduces, however, the fluid free surface frequency increases.

## 4.5. VALIDATION WITH OTHER ANALYTICAL MODELS

The results of the analytical model are compared with results from [12] when the membrane is located at the bottom. Table 4.2 shows a comparison of the coupled frequency results $T_o$ = 500 N/m, m = 1 kg/m. There is a close agreement with both models. A comparison with the refrence [18] when the membrane is located at top. This comparison is very difficult to consider as the equations employed in solving the problem in the reference [18] is quite different. More so, the order of truncation used for the series solution is unknown. However, the values contained in table 4.3 below shows an agreement.

Table 4.2: Comparison of non dimensional coupled frequencies $\mu^2 = \frac{m_m}{T_o}\omega_c^2$ with respect fluid depth (membrane located at bottom)

| | h/a | 1st | 2nd | 3rd | 4th |
|---|---|---|---|---|---|
| Present study | 0.3 | 4.984 | 6.967 | 8.086 | 12.232 |
| Bhuta | 0.3 | 4.676 | 7.140 | 8.807 | 10.129 |

Table 4.3: Comparison of non dimensional coupled frequencies $\mu^2 = \frac{m_m}{T_o}\omega_c^2$ with respect fluid depth(membrane located at the top)

| | h/a | 1st | 2nd | 3rd |
|---|---|---|---|---|
| Present study | 0.1 | - | 4.639 | - |
| Bauer | 0.1 | 2.857 | 5.000 | 6.786 |
| Present study | 0.3 | 4.199 | - | - |
| Bauer | 0.3 | 4.108 | 6.071 | 7.857 |
| Present study | 0.5 | 3.821 | - | - |
| Bauer | 0.5 | 4.286 | 6.428 | 7.857 |

## 4.6. BEHAVIOUR OF THE VIBRATION MODES WITH RESPECT TO THE COUPLED FREQUENCY IN 3-D AT VARYING WATER DEPTH

The vibration mode is simply the vibration pattern of the structure at a particular frequency, this is a very important engineering concept and it is used to predict behaviour of structure due to vibrations. Dealing with the axisymmetric case, the vibration mode of the membrane at different $\frac{h}{a}$ ratio is considered and the vibration mode of the free surfaces is also considered at different $\frac{h}{a}$ ratio. From equations (2.73), (2.83) and (2.87) the vibration modes of the membrane are obtained as seen in figure 4.3a below, the normalized water depth to radius of the membrane ratio is on the abscissa and the deflection of the membrane is on the ordinate axis: there is a considerable change in the behaviour of the vibration at different $\frac{h}{a}$ ratios. There is a strong increase in membrane displacement with lower $\frac{h}{a}$ ratio. Larger displacement indicates more flexibility of the membrane. The free surface vibration modes are given in figure 4.3b below. In figure 4.3b below, there is no considerable changes in the vibration mode of the fluid free surface.

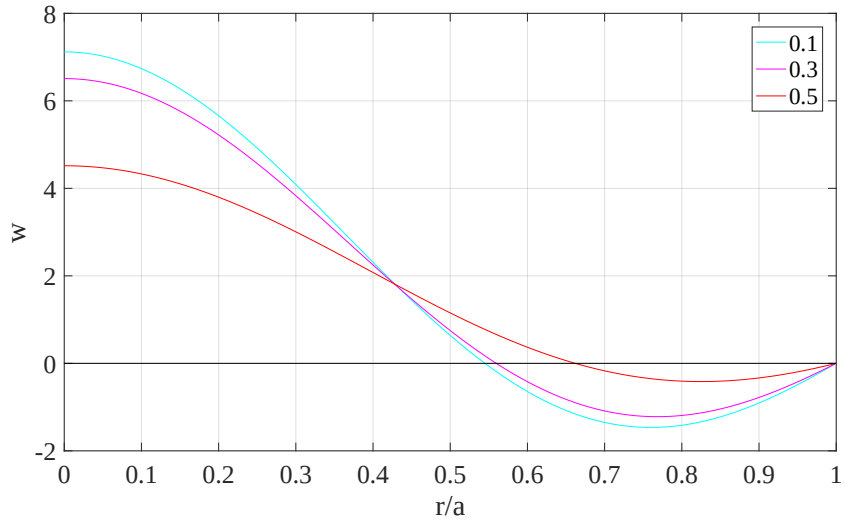


(a) Vibration modes of the membrane at coupled frequency and different $\frac{h}{a}$ , $m$=1 and $n$=0 axisymmetric case

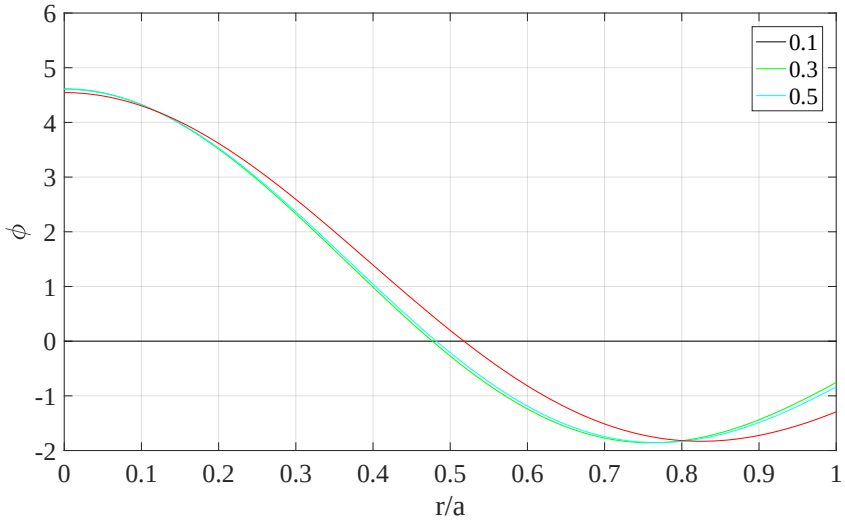


(b) Vibration modes of the fluid free surface mode at coupled frequency and different $\frac{h}{a}$, $m$=1 and $n$=0 axisymmetric case

Figure 4.3: Relationship between vibration modes and changing fluid depth

# 5

# CONCLUSION AND RECOMMENDATION

## 5.1. CONCLUSION

The tasks described in this thesis are a part of a general effort to develop an accurate and efficient computational tool for modelling fluid-structure interaction (FSI). This thesis was focused on the aspect of formulating and solving analytically the coupling phenomenon experienced in an experiment [1] designed to capture fluid-structure interaction modelling. It's main objective was to give an insight to understanding the coupled frequencies and its corresponding vibration modes of the fluid and structure. Therefore, a series of equations were employed, the results analysed and the conclusions reached are elaborated below.

In the 3D case, a Fourier-Bessel series solution was developed to obtain the coupled frequencies. These series solution produced a truncated set of determinant matrices to approximate the solutions in lower frequency regions. The results of the analytical solution showed a close agreement when compared with journal references see tables 4.2 and 4.3. However, this is not case with when the analytical results are compared with experimental and numerical methods developed for modelling the coupling phenomenon of fluid-structure interaction.

## 5.2. RECOMMENDATIONS FOR FUTURE RESEARCH

The problems faced, related to the solving the analytical model and how to make it as accurate as possible are outlined as followed.

- This model should be modified to be able to capture experimental processes such as: viscosity, and surface tension of the fluid. Viscosity is a measure to know the natural decay rate of the coupling phenomenon. These experimental processes if investigated shows a holistic approach to understanding all of the FSI phenomenon.

- The overall equations can be kept as it is. However, the order of the Fourier-Bessel series solution should be increased. This in turn increases the elements of the determinant matrix. This needs to be investigated to know the behaviour of higher modes. See equations (2.91) and (2.156).

- A comparison of the results of this study with another analytical method, for example, using energy methods can be employed to verify the analytical solution.

# BIBLIOGRAPHY


[1] L. Rizos, *Reduced - complexity experiment for validating Fluid-Structure Interaction in ComFLOW*, Ph.D. thesis (2016).

[2] K. Rajput, *Vibrations of Structures,* (2003).

[3] M. Ross, *SD-04:Vibrations of Circular Membrane - Eigensolutions,* (2017).

[4] P. Kelly, *Solid Mechanics Part II,* (2008).

[5] A. Sondipon, *Models, Verification, Validation, Identification and Stochastic Eigenvalue Problems.* in *Mechanical Vibration: Where Do We Stand?* (CISM Udine, 2007) pp. 321–388.

[6] T. Helder, Joop; Bunnik, *ComMotion,* (2014).

[7] J.-M. Korobkin, Alexander; Vanden-Broeck and E. Parau, *The mathematical challenges and modelling of hydroelasticity,* Philosophical Transactions of The Royal Society A Mathematical Physical and Engineering Sciences (2011), 10.1098/rsta.2011.0116.

[8] A. W. Leissa, *Vibration of plates,* Ohio State Univ Columbus , 362 (1969), arXiv:arXiv:1011.1669v3 .

[9] L. Leniowska, *Vibrations of Circular Plate Interacting With an Ideal,* Archieves of Acoustics **441**, 427 (1999).

[10] M. Moosrainer and H. Fleischer, *Interaction of a Membrane With an Enclosed and Surrounding Fluid — Fem / Bem Coupling,* (2017).

[11] M. Amabili, *Vibrations of Circular Plates Resting on a Sloshing Liquid: Solution of the Fully Coupled Problem,* Journal of Sound and Vibration **245**, 261 (2001).

[12] P. G. Bhuta and L. R. Koval, *Coupled oscillations of a liquid with a free surface in a tank having a flexible bottom,* Zeitschrift füur angewandte Mathematik und Physik ZAMP **15**, 466 (1964).

[13] H. Bauer, Chiba, and M., *Viscous Hydroelastic Vibrations in a Cylindrical Container With an Elastic Bottom,* Journal of Sound and Vibration **247**, 33 (2001).

[14] W. S. Wermelin and I. Buchberger, *Modelling of Drums*, Ph.D. thesis (2015).

[15] T. M. Juliano, *Newark, New Jersey*, Ph.D. thesis (1970).

[16] W. Rosenheinrich, *Tables of Some Indefinite Integrals of Bessel Functions,* in *Treaties on Bessel Function* (2016) p. 457.

[17] P. M. Morse, *Vibration And Sound.pdf*, 2nd ed., edited by G. Harnwell (McGraw-Hill Book Company INC., New York, 1948) p. 485.

[18] H. Bauer, *Coupled frequencies of a liquid in a circular cylindrical container with elastic liquid surface cover,* **180**, 689 (1995).

# Appendices

# A

# ANALYSIS OF FLUID-MEMBRANE FREQUENCY IN 3D: IMPLICITPLOT

To understand how the coupling equation is formed, it is expedient to understand that the order determinant matrix. With an increasing order of determinant matrix gives increasing accuracy. However, solving this determinant implicitly (*when two variables do not have an expression to explain its relationship*) gives another idea of what the coupled frequencies are. An analytical software – MAPLE was used to solve the linear equations and make implicit plots of the determinant against the unknown coupled frequencies. These implicit plots are another way to verify the results of the coupled frequencies. There is a close agreement with the implicit plot and the general plot and almost the same values with higher coupled frequencies. The pairing behaviour of coupled frequencies to mode shapes are as well observed and concluded that it is only a numerical problem in finding the roots of the equation. Thus, the roots close to each other exhibits closely related mode shapes. A noticeable problem was observed when the x-axis increases. This problem is due to how MAPLE works and not the equations, hence, truncating the infinite number of frequencies to a finite $m$ by $m$ matrix and whose determinant are easy to solve. The implicit plots of the are shown below in the figure A.1 below.

From the figure A.1 above, the roots are seen to be one distinct(*constant*) value, and as such, the coupled frequencies are clearly seen.

Table A.1: Comparison of implicit and general plot coupled frequencies with $h/a$ = 0.3, $T_o$=500 $N/m$, $m$=1$kg/m$, $a$=1$m$ membrane located at the bottom

| s/n | 1 | 2 | 3 | 4 | 5 |
|---|---|---|---|---|---|
| Implicit Frequency (rad/s) | 6.142 | 6.964 | 8.066 | 12.242 | 128.243 |
| Frequency (rad/s) | 4.984 | 6.967 | 8.086 | 12.232 | 128.783 |
| difference(%) | 81.146 | 0.0431 | 0.248 | 0.999 | 0.421 |

It can be seen from table A.1 values with difference also close to zero shows a close agreement and it indicates that an actual crossing is present and not an asymptotic anomaly.

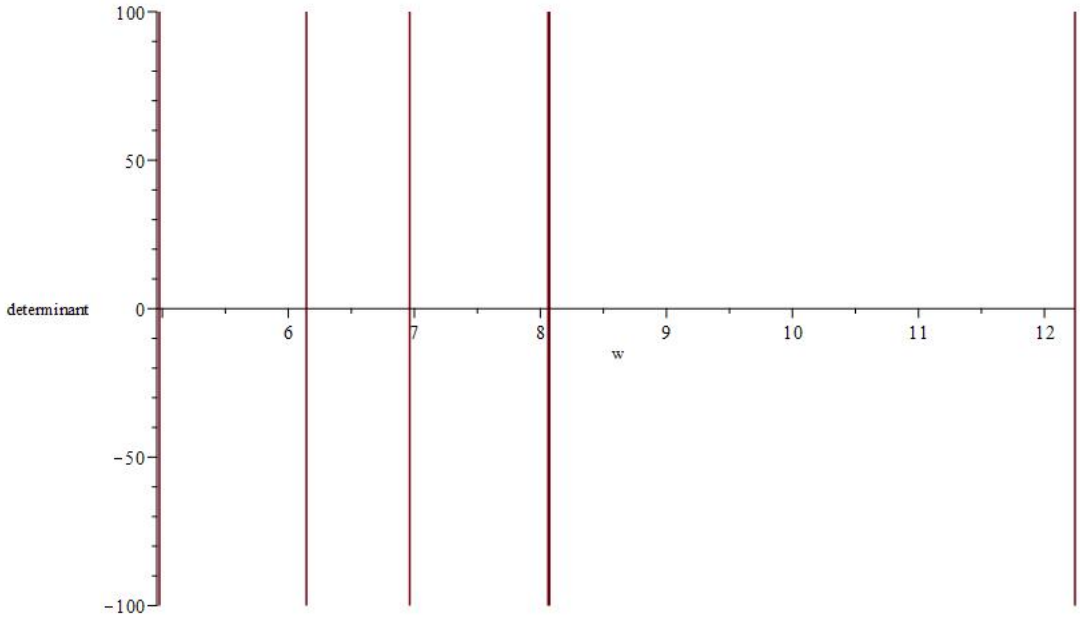


Figure A.1: Implicit plot of determinant to obtain coupled frequencies with $h/a$ = 0.3, $T_o$=500 $N/m$, $m$=1$kg/m$, $a$=1$m$

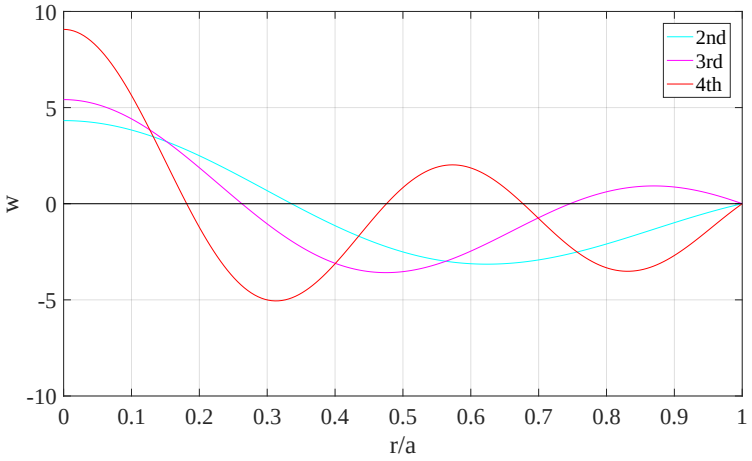


(a) Membrane modes – implicit solver

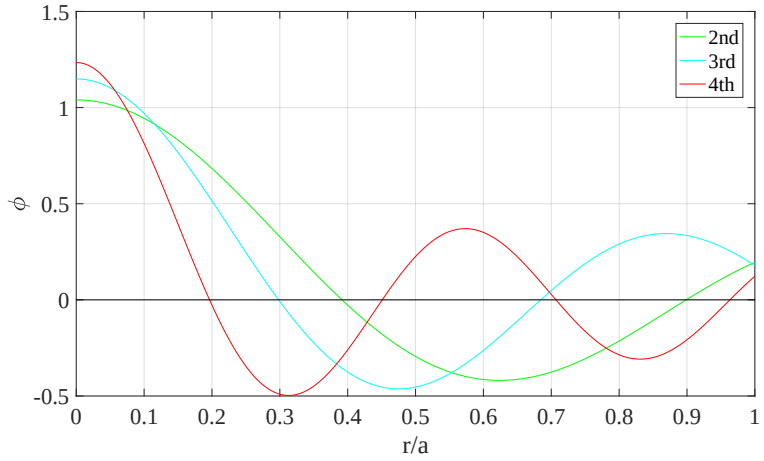


(b) Fluid free surface modes – implicit solver

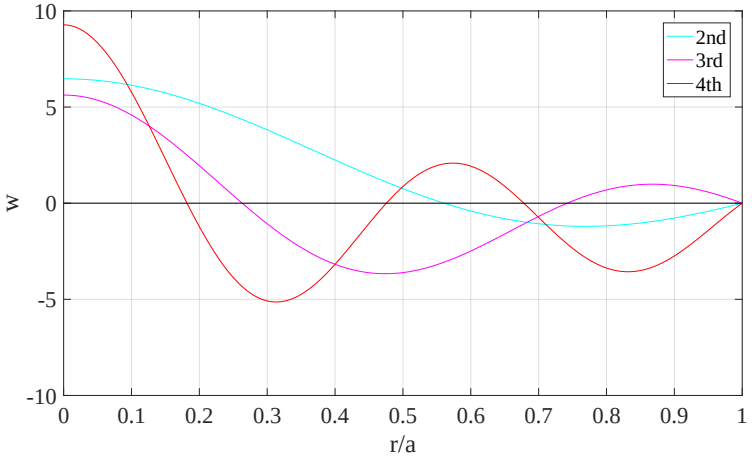


(c) Membrane modes – complete solution

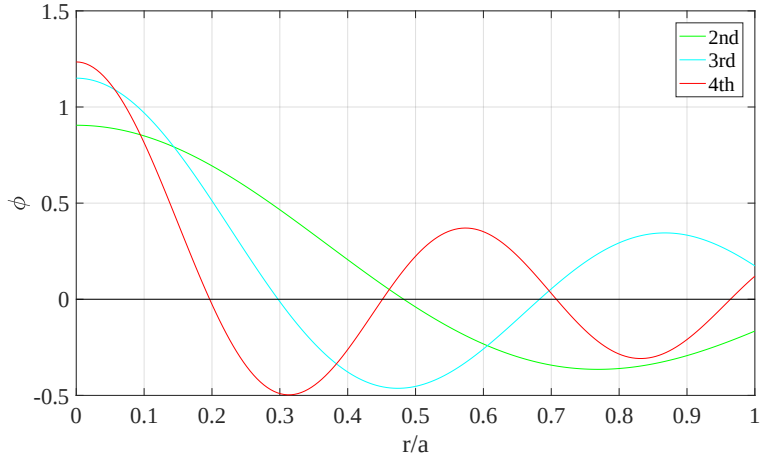


(d) Fluid free surface modes – complete solution

Figure A.2: Comparison of vibration modes of the membrane and free surface at first three coupled frequencies for axisymmetric case with $h/a = 0.3$, $T_o$=500 $N/m$, $m$=1$kg/m$, $a$=1$m$ for implicit solver and general solution

# B

# Some Visualization of Vibration Modes of a Circular Membrane *In Vacuo*

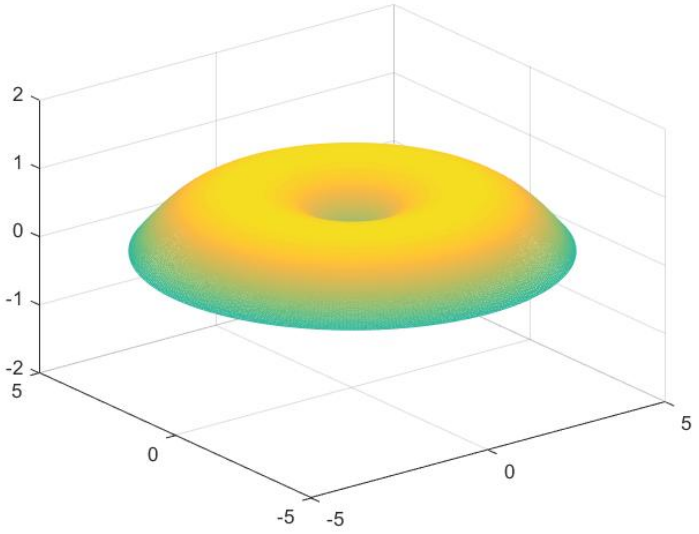


(a) Vibration mode for n=0, m=1

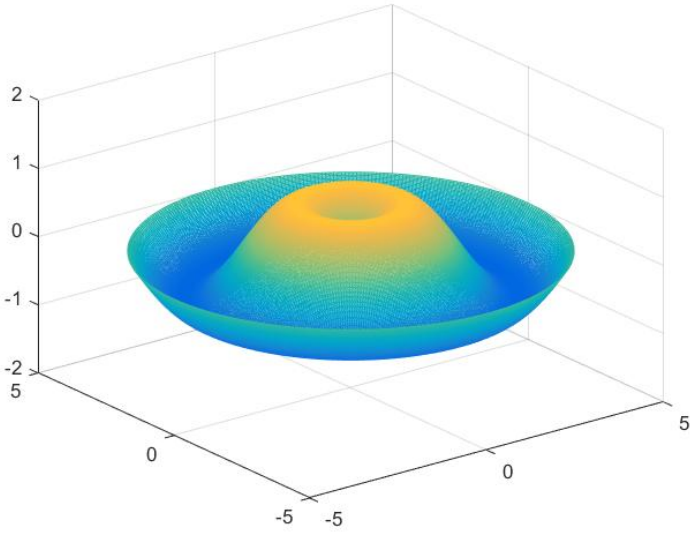


(b) Vibration mode for n=0, m=2

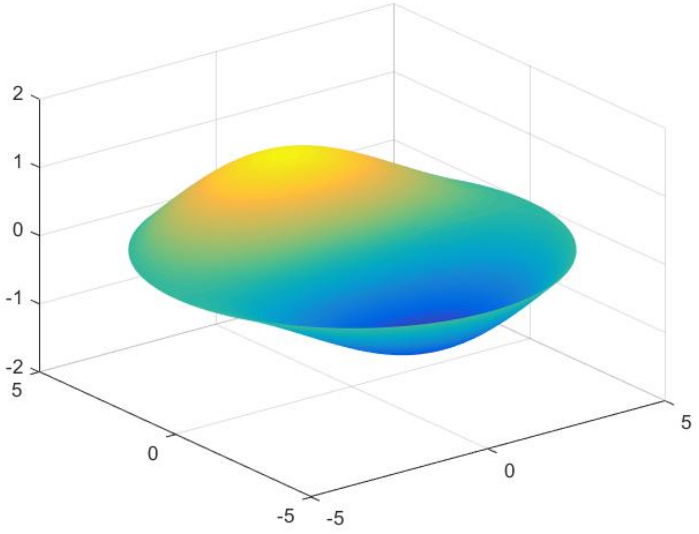


(c) Vibration mode for n=1, m=1

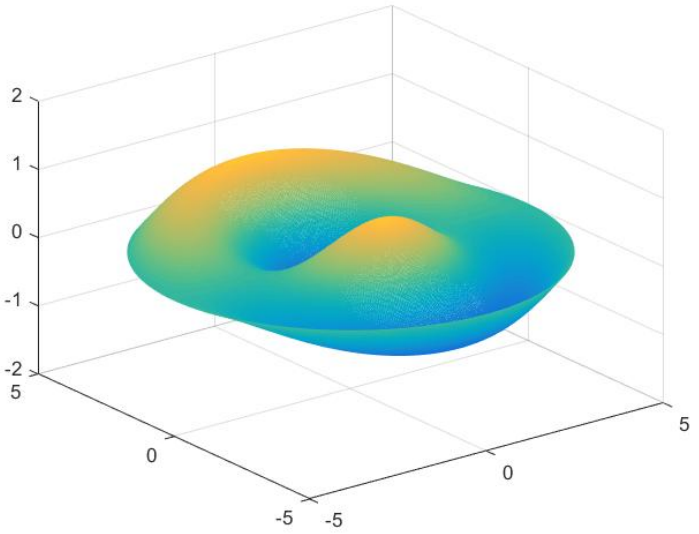


(d) Vibration mode for n=1, m=2